

PETROPHYSICAL AND STRUCTURAL ANALYSIS OF LOWER  
GORU FORMATION, SOUTHERN SINDH MONOCLINE, LOWER  
INDUS BASIN, PAKISTAN



Anees Sabir  
(01-262181-001)

A thesis submitted in the fulfillment of the requirements for the award of  
degree of Master of Science (Geology)

Department of Earth and Environmental Sciences

BAHRIA UNIVERSITY ISLAMABAD

FEBRUARY 2021

## **Approval for Examination**

**Scholar's Name:** Anees Sabir

**Registration No:** 56122

**Program of Study:** MS Geology

**Thesis Title:** Petrophysical and Structural Analysis of Lower Goru Formation,  
Southern Sindh Monocline, Lower Indus Basin, Pakistan

It is to certify that the above scholar's thesis has been completed to my satisfaction and, to my belief, its standard is appropriate for submission for examination. I have also conducted a plagiarism test of this thesis using HEC prescribed software and found a similarity index of 8% that is within the permissible limit set by the HEC for the MS degree thesis. I have also found the thesis in a format recognized by the BU for the MS thesis.

Principal Supervisor's Signature: \_\_\_\_\_

Date: \_\_\_\_\_

Name: \_\_\_\_\_

**Author's Declaration**

I, Anees Sabir hereby state that my MS thesis titled “Petrophysical and Structural Analysis of Lower Goru Formation, Southern Sindh Monocline, Lower Indus Basin, Pakistan” is my work and has not been submitted previously by me for taking any degree from this university (Bahria University) or anywhere else in the country/world.

At any time if my statement is found to be incorrect even after my graduation, the University has the right to withdraw/cancel my MS degree.

Name of Scholar: \_\_\_\_\_

Date: \_\_\_\_\_

### **Plagiarism Undertaking**

I, solemnly declare that research work presented in the thesis titled “Petrophysical and Structural Analysis of Lower Goru Formation, Southern Sindh Monocline, Lower Indus Basin, Pakistan” is solely my research work with no significant contribution from any other person. Small contribution/help wherever taken has been duly acknowledged and that complete thesis has been written by me.

I understand the zero-tolerance policy of the HEC and Bahria University towards plagiarism. Therefore, I as an author of the above-titled thesis declare that no portion of my thesis has been plagiarized and any material used as the reference is properly referred/cited.

I undertake that if I am found guilty of any formal plagiarism in the above-titled thesis even after awarding of MS degree, the university reserves the right to withdraw/revoke my MS degree and that HEC and the University have the right to publish my name on the HEC / University website on which names of scholars are placed who submitted plagiarized thesis.

Scholar / Author’s Sign: \_\_\_\_\_

Name of the Scholar: \_\_\_\_\_

## ABSTRACT

The research area is from the Badin Block of the Lower Indus Basin, Sindh, Pakistan. The area is tectonically stable with a monoclinical structure commonly known as Sindh monocline. The Lower Indus basin tectonically represents an extensional regime. The Lower Indus basin contributes 40% oil and approximately 70% gas of the country's total production. Badin area is at the forefront of Pakistan's production with 307 wells drilled to date which explains the hopeful hydrocarbon prospect in this area. The purpose of this study is to apply reservoir rock physics fundamentals for understanding the reservoir architecture for hydrocarbon potential. In this regard, two wells Jabo-1 and Jabo-5 were selected using petrophysical and seismic approach in the Cretaceous Lower Goru Formation, a reservoir of both the wells. In the Badin area, the rock formations show a complex deformation history, which can be classified into three major events 1) Early Cretaceous (Basal Sand to Upper Goru) 2) Middle to Late Cretaceous (Basal Sand to Upper Goru) and 3) Post Paleocene (uplifting and doming). Based on the petrophysical analysis, zones were selected for the reservoir at different depths. The effective porosity for both wells ranged from 5.49% to 7.15% with a water saturation ranging from 45.24% to 80.21%. Cross plots generated from different parameters confirm that there are only three types of lithologies in the selected zone of reservoir that are hydrocarbon sands, brine sands, and shales. Petrophysical analysis confirms an increase in the reservoir quality towards the southern part of the oil field. Seismic interpretation revealed the existence of horst and graben structures in the subsurface. Five horizons were picked on the seismic sections by incorporating well data. The generated contour maps depth indicates that the reservoir of the area is dipping in the southwest direction with the major orientation of faults in the northwest direction.

## **ACKNOWLEDGEMENTS**

In the name of Allah, the most beneficent and most merciful. I am thankful to Allah Almighty for blessing me to complete my degree and accomplish my thesis.

I am thankful and obliged to my supervisor Prof. Tahseenullah Khan, Department of Earth and Environmental Sciences, School of Engineering and Applied Science, Bahria University Islamabad for his guidance and encouragement to complete my thesis work. I am thankful to Dr. Said Akbar Khan, the HoD E&ES department for facilitating this research. Thanks are also extended to Dr. Nosheen Sahir, Assistant Professor who selected the topic and agreed to supervise me before she left the university. I am also thankful to the PGP coordinator, Cluster Head and the internal and external examiners who critically reviewed my thesis and offered a fruitful suggestion. Thanks are also extended to Muhammad Zeeshan Shahid, Weatherford, M. Ali, Senior Geologist, Prospect generation, OGDCL Islamabad, and my friends for technical support and guidance. DGPC and LMKR are thanked for providing me data for my research work.

Last but not the least, I am thankful to my parents and friends for their support during my entire endeavor for the completion of my MS program.

## TABLE OF CONTENTS

CHAPTER	TITLE	PAGE
	<b>ABSTRACT</b>	v
	<b>ACKNOWLEDGMENT</b>	vi
	<b>TABLE OF CONTENTS</b>	vii
	<b>LIST OF FIGURES</b>	x
	<b>LIST OF TABLES</b>	xiii
<b>1</b>	<b>INTRODUCTION</b>	1
	1.1 General Statement	1
	1.2 Petroleum System	2
	1.3 Hydrocarbon Potential	2
	1.4 Exploration History	3
	1.5 Literature Review	5
	1.6 Objectives	5
<b>2</b>	<b>GEOLOGY AND TECTONICS</b>	7
	2.1 General Tectonics	7
	2.2 Structural Setting	8
	2.3 Stratigraphy	8
<b>3</b>	<b>MATERIALS AND METHODOLOGY</b>	12
	3.1 Wells Selection	12
	3.2 Jabo-01	14
	3.3 Jabo-05	14

3.4	Petrophysical Analysis	15
3.5	Quality check	16
3.6	Selection of zones	17
3.7	Reservoir Evaluation	17
3.7.1	Volume of Shale	17
3.7.2	Porosity Measurement	18
3.7.2.1	Density Porosity (DPHI)	18
3.7.2.2	Neutron porosity (NPHI)	19
3.7.2.3	Sonic porosity	20
3.7.2.4	Average (APHI) and effective porosity (EPI)	20
3.7.3	Spontaneous Potential	21
3.7.4	Resistivity of water (Rw)	22
3.7.5	Water saturation (Sw) and hydrocarbon saturation (Sh)	26
3.8	Seismic Data	26
3.9	Data Quality Check	27
3.10	Base Map	27
3.11	Seismic approaches	28
3.11.1	Structural interpretation	28
3.11.2	Stratigraphic Interpretation	28
3.12	Well to Seismic Tie	29
3.13	Synthetic Seismogram	29
3.14	Contour Maps	29
<b>4</b>	<b>PETROPHYSICAL INTERPRETATION</b>	<b>30</b>
4.1	Jabo 01	30
4.2	Jabo 05	35
4.3	Correlation	39
4.4	Lithological Identification	42
4.4.1	Lithological Identification from Rock Physics	44



4.4.1.1	Acoustic Impedance and $V_p/V_s$	43
4.4.1.23	Mu-Rho and Density	45
4.4.1.3	Incompressibility and Mu-Rho	46
<b>5</b>	<b>SEISMIC INTERPRETATION</b>	<b>47</b>
5.1	Seismic lines used for interpretation	47
5.2	Control Line	48
5.3	Faults Interpretation	48
5.4	Horizon Interpretation	48
5.5	Seismic Line Interpretation	49
5.6	Synthetic Seismogram	50
5.7	Contour Maps	63
5.7.1	Time contour maps	63
5.7.2	Depth contour maps	63
5.8	Contour maps Interpretation	63
5.8.1	Top Upper Goru Formation	63
5.8.2	Top Lower Goru	67
	<b>CONCLUSIONS</b>	<b>70</b>
	<b>REFERENCES</b>	<b>72</b>

## LIST OF FIGURES

<b>FIGURE NO</b>	<b>TITLE</b>	<b>PAGE</b>
1.1	Pie chart showing the comparison of crude oil production of Pakistan from all regions (HDIP, 2016)	4
1.2	Pie chart showing a comparison between gas productions of all regions of Pakistan (HDIP, 2016).	4
2.1	Geological and Basin map of Pakistan showing study area (After Hanif et al, 2012)	9
2.2	Structural setting of the Southern Indus Basin (modified after H.A. Raza et al., 1990).	10
2.3	Generalized stratigraphic sequence in the southern Indus basin (modified after Shah, 1977; Raza et al., 1990).	11
3.1	Generalized map showing the location of Jabo field of the Badin Block	13
3.2	Schlumberger Gen-9 chart.	23
3.3	Schlumberger SP-1 chart.	24
3.4	Schlumberger SP-2 chart.	25
3.5	Base map of selected seismic lines.	27
4.1	The environment of deposition of Lower Goru Formation in Jabo-01 well.	31
4.2	Petrophysical interpretation of Lower Goru Formation in Jabo-01	33
4.3	The environment of deposition of Lower Goru Formation in Jabo-05 well.	34
4.4	Petrophysical interpretation of Lower Goru Formation in Jabo-05	37

4.5	Correlation of Lower Goru Formation in Jabo-01 and Jabo-05	40
4.6	Correlation of environment of deposition of Lower Goru Formation in Jabo-01 and Jabo-05.	41
4.7	Cross plot between neutron and density for lithological identification.	42
4.8	Cross plot between P-imp and VpVs ratio for well Jabo-05 and effective porosity is shown in the color legend.	44
4.9	Cross plot between density and MuRho for well Jabo-05 and gamma ray is shown in the color legend.	45
4.10	Cross plot between MuRho and Lambda-rho for well Jabo-05 and effective porosity is shown in the color legend.	46
5.1	Synthetic seismogram in Jabo-01	51
5.2	Synthetic to seismic tie on line GPK86-1200.	52
5.3	Seismic line GPK86-1200.	53
5.4	Structural interpretation of seismic line GPK86-1200.	54
5.5	Structural and stratigraphic interpretation of seismic line GPK86-1200.	55
5.6	Interpreted seismic line GPK86-1202.	56
5.7	Interpreted seismic line GPK85-937.	57
5.8	Interpreted seismic line GPK85-0958	58
5.9	Interpreted seismic line GPK92-1678.	59
5.10	Interpreted seismic line GPK85-KH04.	60
5.11	Interpreted seismic line GPK85-KH06.	61
5.12	Interpreted seismic line GPK85-KH01.	62
5.13	Time contour map of Upper Goru Formation.	65

5.14	Depth contour map of Upper Goru Formation.	66
5.15	Time contour map of Lower Goru Formation.	68
5.16	Depth contour map of Lower Goru Formation.	69

**LIST OF TABLES**

<b>TABLE</b>	<b>TITLE</b>	<b>PAGE</b>
3.1	Formation tops and thicknesses in Jabo-01	14
3.2	Formation tops and thickness in Jabo-05	15
3.3	Well logs used for petrophysical interpretation	16
3.4	List of seismic lines used for interpretation.	26
4.1	Reservoir summary for Jabo-01	34
4.2	Reservoir summary for Jabo-05.	38
4.3	Reservoir summary comparison	39
5.1	List of seismic lines used for interpretation	47

## LIST OF ABBREVIATIONS

$A_{PHI}$	Average porosity
AR	Archie's.
BP	British petroleum
DGPC	Directorate general of petroleum concessions
$D_{PHI}$	Density porosity
DT	Sonic log
$E_{ij}$	potential of the liquid junction
$E_m$ .	potential of membrane potential
$E_{PHI}$	Effective porosity
$E_{total}$ .	total SP potential
G.G	Geothermal Gradient
GR	Gamma ray
$GR_{min}$	Minimum value of GR
$GR_{max}$	Maximum value of GR
IGR	Gamma ray index
LLS	Laterolog shallow
LLD	Laterolog deep
LMKR	Land mark resource
MSFL	Micro resistivity log
Mu-rho	Rigidity
NPHI	Neutron log
$N_{PHIE}$	Neutron porosity
QC	Quality check
RHOB	Density log

$R_{mf}$	Resistivity of mud filtrate
$R_w$	Resistivity of water
$S_h$	Saturation of hydrocarbon
SP	Spontaneous potential
$S_{phi}$	Sonic porosity
$S_w$	Saturation of water
TD	Total depth
$T_f$	Formation temperature
UTP	Union Texas Pakistan
$V_p$	P wave velocity
$V_s$	S wave velocity
$V_{clean}$	Volume of clean
$V_{sh}$	Volume of shale
$\Phi$	Porosity
$\lambda\rho$	lambda-rho
$\mu\rho$	mu-rho
$\rho$	Density
$\rho_{ma}$	Density of matrix
$\rho_f$	Density of fluid
$\Delta t$	Travel time from sonic log
$\Delta t_{ma}$	Travel time in matrix
$\Delta t_f$	Travel time in the formation fluid

## **CHAPTER 1**

### **INTRODUCTION**

#### **1.1 General Statement**

The Badin Block is situated in the Lower Indus Basin, in the south of the Sindh province, Pakistan. It is approximately 160 km in the east from Karachi city. The area covered by the concession is about 7,650km<sup>2</sup>. The research area lies in Badin block Southern Indus Basin which is situated on longitude from 68° 11'E to 68° 47'E and on latitude from 24°06'N to 25° 02'E. Two wells from the Jabo field of the block (Jabo-01 with latitude 24°21'31.13 and longitude 68°33'16.20' and Jabo-05 of latitude 24°21'8.49" and longitude 68°33'16.00) were used for interpretation. It covers an area of 1265.3km<sup>2</sup> is bounded by Hyderabad district in the north and Tharkarparkar district on the east, whereas it is bordered by Badin district borders on the western side and by the Arabian Sea in the south.



## **1.2 Petroleum System**

The early Cretaceous Sembar Formation is thought to be the major source rock of the Badin area whereas Early Cretaceous clastic rocks of the Lower Goru Formation are the major reservoir (Ahmed et al., 2014). Traps of this area are mainly tilted fault blocks and associated with normal faults of the Early Paleocene and Late Cretaceous time rift phase (Memon et al, 1998). Shale and impermeable marl sequence of Upper Goru Formation is acting as caprock in this area. Deccan Basalts of the Early Paleocene are thought to be the cause of hydrocarbons generation from the underlying source rocks (Goru and Sembar Formation) because of high temperature (Zaigham and Malick, 2000). Major reserves found in the Badin area are in the Upper Sand (B Sands) of the Lower Goru Formation contributing 60% to the total reserves (Ebdon et al., 2004).

## **1.3 Hydrocarbon Potential**

Oil of Badin Block is very sweet and paraffinic of API gravity ranging from 33 to 56. It is light in the northern and central part while heavy and waxy in the southern part (Ahmed et al., 2014). The oil reservoir depth in this block ranges from 609 m to 14114m. Bhatti Bobby Golarchi, Tando Alam, Pasakhi, and Khaskeli are the most productive hydrocarbon fields of this area. Badin Block area is more favorable for both oil and gas whereas Kirthar hills and mountains and their adjacent areas are only known for gas (Boyd, 1994). About 12 trillion cubic feet of gas reserves and more than 100 million barrels of oil have been discovered in the Lower Indus Basin whereas the Badin area contributes to more than 90% of oil production (Ahmed et al., 2014). The oil operators in this region are OGDCL (Oil and Gas Development Company Limited) and United Energy Pakistan Limited. Khaskeli was the first and also the largest oil field in the Badin area (Petzet et al., 1997).

## 1.4 Exploration History

Stanvoc Oil and Gas Exploration Company actively started exploration for the first time in the study area from 1956 to 1961. Several dry wells were drilled with some hydrocarbon shows. These wells failed because their target was off structure due to the very low data control and poor seismic quality of formations below Deccan Volcanics (Petzet et al., 1997). There was no exploration activity till UTP (Union Texas Pakistan) and OGDCL acquired an exploration lease of the concessions of the region from DGPC in April 1977. The UTP (Union Texas, Pakistan) group began exploration in the study area on the 8,637 km<sup>2</sup> (Ahmed et al., 2014)

The Khaskeli was the first UTP group discovery in 1981 from the Upper Sand interval, opening a new play for oil exploration in Pakistan. The Golarchi is the first gas discovery from the Lower Goru Upper Sand. Later on, 104 exploratory wells were drilled through up to 1997 achieving a milestone of 47 discoveries along with 57 dry holes. Seismic data quality was poor in the early years, but acquisition and interpretation gave excellent results. In 1997 11 exploratory wells were planned in Badin exploration. The plan included Tarai Deep-3 for testing of an unexplored play of deeper Chiltan Formation of Jurassic Formation along with the first 3D seismic acquisition at Tangri and South Buzdar fields in the northern side of the block. South Mazari, Mazari, and Laghari fields are under secondary recovery and responding well (Hargreave, 1990). Most oil reservoirs are water drives with around 50% recovery expected, and most gas fields are depletion drives with close to 70% recovery expected (Hargreave, 1990). Comparison of overall original recoverable reserves of crude oil of Pakistan and Southern Sindh Monocline is shown in Pie Chart figure 1.1 while the Pie Chart is shown in figure 1.2 showing a comparison of overall gas reserves of Pakistan and Southern Sindh Monocline (HDIP, 2019).

According to the annual report of 2019 sum of recoverable reserves of Pakistan is 1102 million US barrels of oil while 40% (434 million) of all reserves were reported for the Southern Sindh Monocline region (figure 1.1). The total calculated recoverable gas reserves for Pakistan is 55.63 TCF out of which 7.63 TCF (13%) fall in this region (HDIP, 2019).

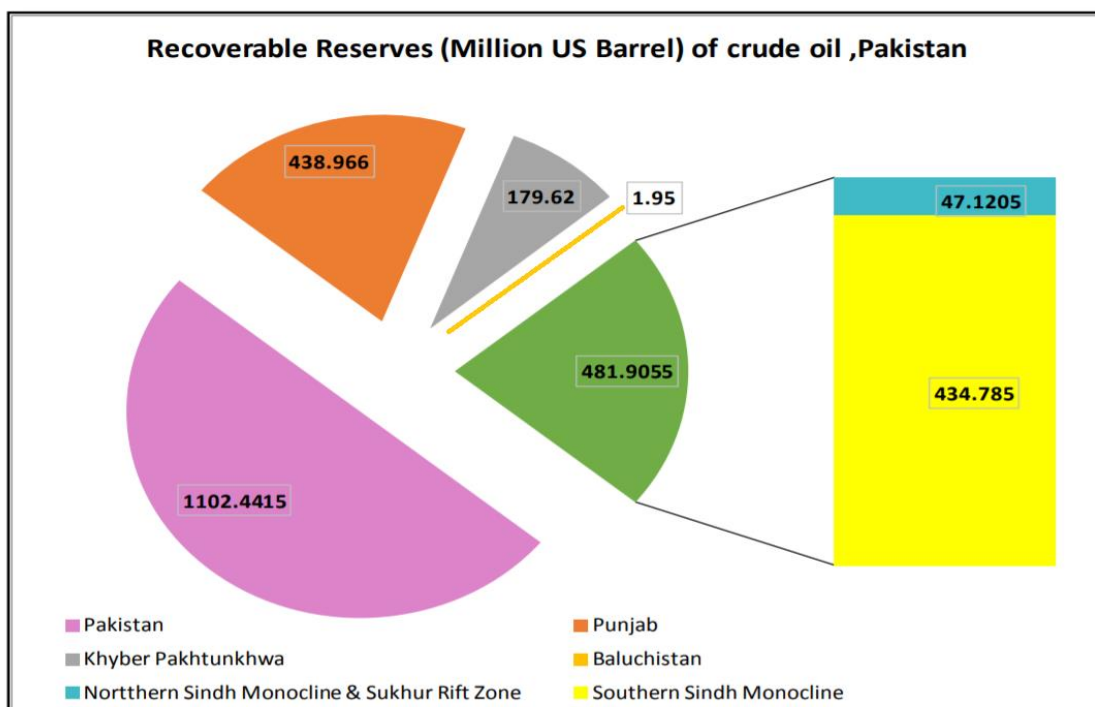


**Figure 1.1** Pie chart showing the comparison of crude oil production of Pakistan from all regions (HDIP, 2016)

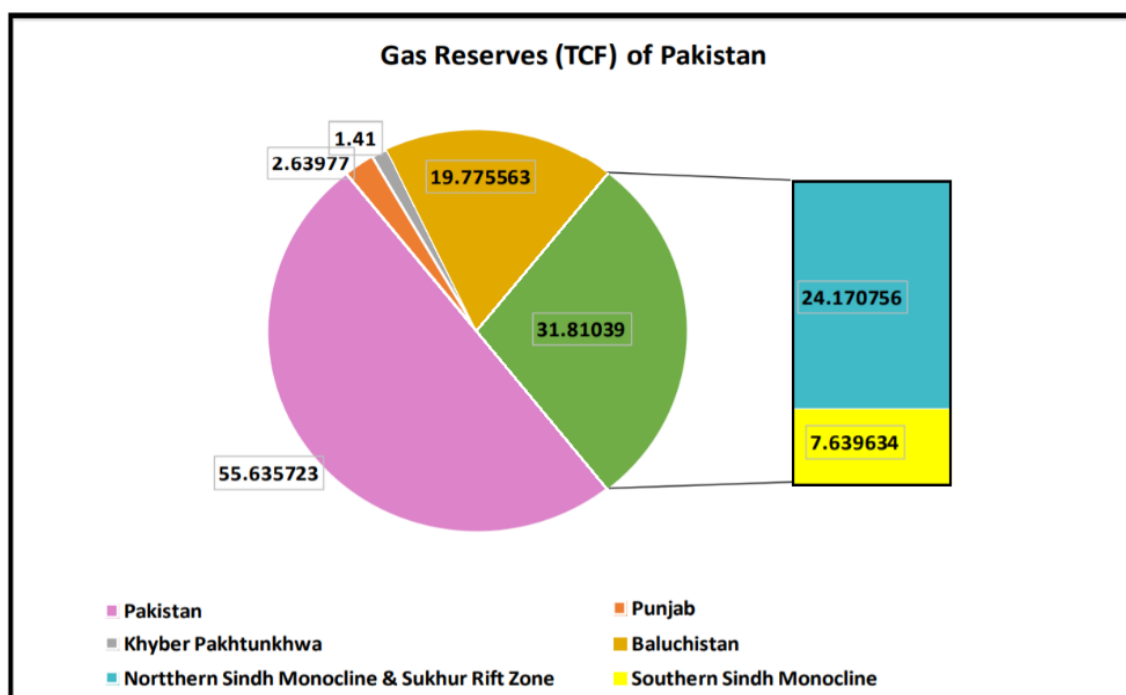


**Figure 1.2** Pie chart showing a comparison between gas productions of all regions of Pakistan (HDIP, 2016).

## **1.5 Literature Review**

Sindh Monocline is a hydrocarbon-rich extensional basin of Pakistan (Kadri, 1995). As numerous discoveries of hydrocarbons are associated with the Cretaceous tectonic episodes of the Indian plate, consequently the Indus basin remained a focused region to petroleum exploration companies in Pakistan (Ahmed et al., 2014).

Ahmed et al., (2004) investigated oil and gas breakdown, distribution, and shallow and deep gas in the Badin Block. The gas of the Badin Block is produced due to oil breakdown along with the direct breakdown of gas-prone kerogen (Ahmed et. al., 2018). Also, the faults reactivation provided secondary migration of oil of deeper reservoir (Lower Goru B-sands of Lower Goru) to the shallow reservoir (Lower Goru Upper Sands). This provides an understanding of the structure, migration pathways, traps, and timings by correlation of data of different fields of the Badin area (Ahmed et al., 1999).

Badin Blocks have confirmed reserves of 100MMboe being produced from over 50 fields. More than 50% of reserves and production is from Lower Goru Formation in the country (Ebdon et al., 2004). It is the main reservoir in the area but its units are not developed everywhere. Stratigraphic barriers were also predicted in the block (Ebdon et al., 2012).

## **1.6 Objectives**

Following are the objectives of this research:

- 1) Determination of environment of deposition.
- 2) Reservoir quality from the petrophysical analysis.

- 3) To study reservoir facies quality by correlating petrophysical properties of selected wells.
- 4) Lithological identification from cross plots.
- 5) To find out subsurface structure and its extension in the area by using seismic techniques.

## CHAPTER 2

### GEOLOGY AND TECTONICS

#### 2.1 General Tectonics

Pakistan is subdivided into two main basins based on the genesis and tectonic history which are Indus and Baluchistan Basin (Kadri, 1995). These basins are further divided into sub-basins due to their respective tectonic events. Indus basin is divided into Lower Indus Basin (Southern and Central Indus Basin) and Upper Indus Basin (figure 2.1).

Rift zone developed due to extension in the Lower Indus Basin and resulting in the formation of Sargodha Highs which is the boundary between the Upper and Lower Indus Basin (Kadri, 1995). The rate of extension is higher in the western part of the basin thus the study area is dominated by normal faults which is the eastern part of the Lower Indus Basin (Hedley et al., 2001). Figure 2.1 shows the setting of sedimentary basins of Pakistan. The Badin Block has undergone three major structural episodes that have played a vital role in the petroleum system of the block, e.g., rifting in Cretaceous and Late Jurassic time, shear modification in the Middle Cretaceous and Late Tertiary inversion (uplift and down coming; Zaigham and Mallick, 2000).

## **2.2 Structural Setting**

The Badin Block is situated on the southwestern edge of the Indian plate. It extends to the south of Khairpur High and reaches out into the Arabian Sea. Whereas, Tharparkar High and Kirthar fold and Thrust belt lie in east and west respectively (figure 2.2). As the block area was distal to the main deformation zone, so deformation is not intense (Raza et al., 1990). Subsequently whole Southern Basin show extensional tectonics and therefore, normal faults. (Kemal et al., 1992).

## **2.3 Stratigraphy**

The Lower Indus Basin has rocks ranging from the early Triassic to Recent alluviums (figure. 2.3). The stratigraphic succession of the Lower Indus basin comprises rocks ranging from Pleistocene Siwalik to Triassic/Jurassic carbonates while the basement rocks of Precambrian are exposed in the southeastern edge of the basin at Nagar Parkar (Kazmi, and Jan, 1997). Sediment thickness increases westward. The formations of Cretaceous age (Pab, Mughalkot, Parh) formations pinch out towards the eastern part of the Lower Indus basin but this sequence is missing in the Thar platform (Raza et al., 1977). The main reservoir rocks are Pub, Mughalkot and Lower Goru and Sembar formation is acting as a source in the basin (Kadri, 1995).

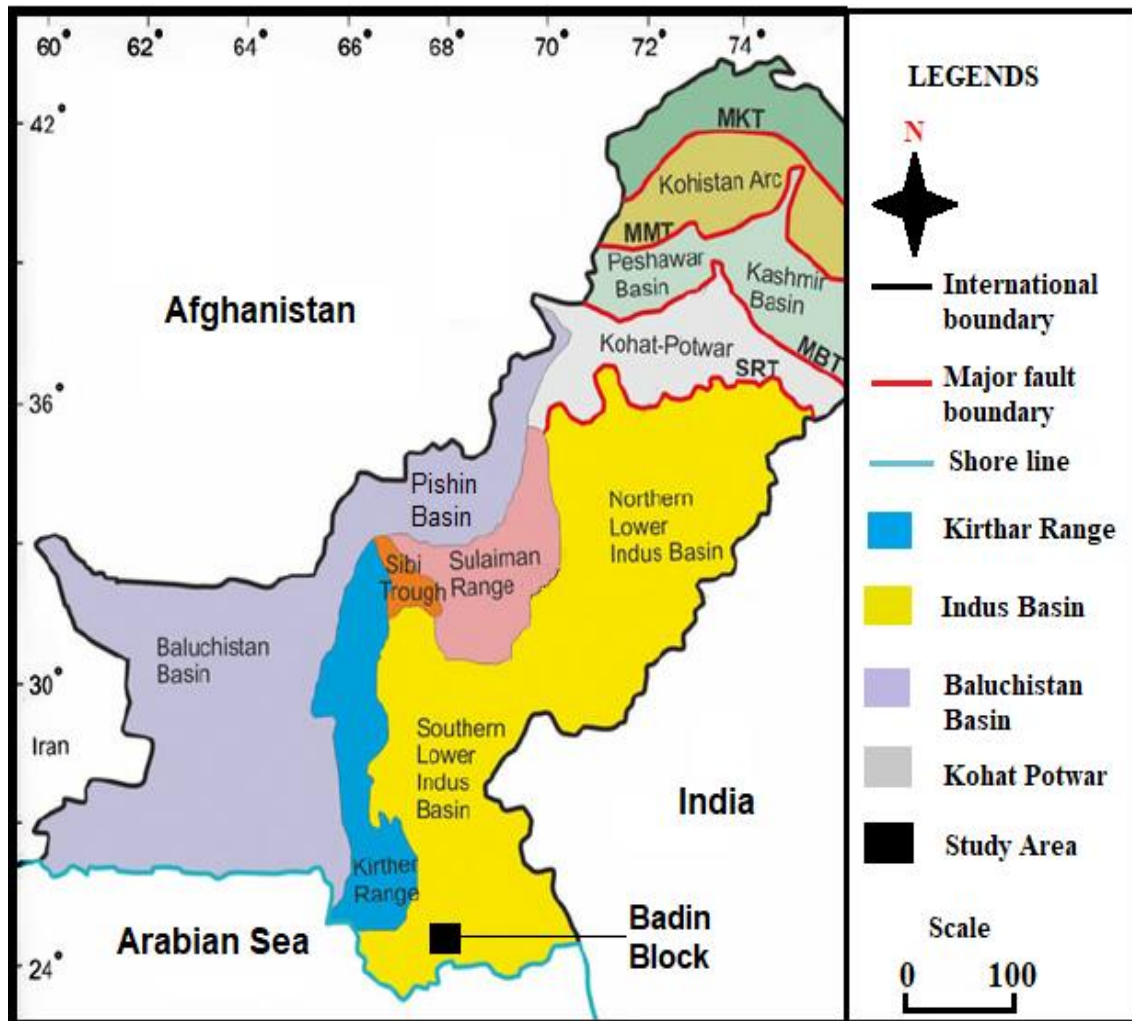


**Figure 2.1** Geological and Basin map of Pakistan showing study area (after Hanif et al., 2012)



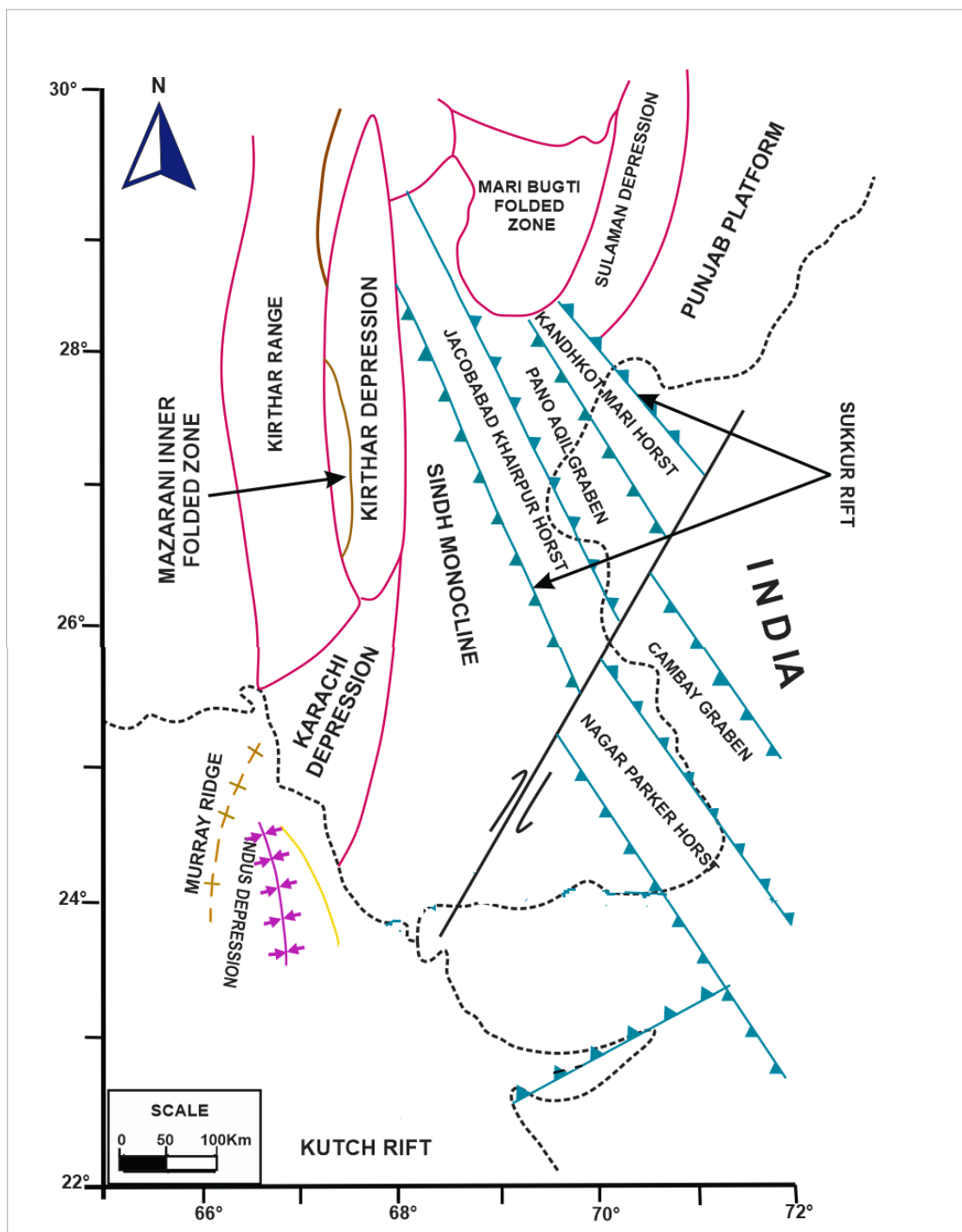


**Figure 2.2** Structural setting of the Southern Indus Basin (modified after Raza et al., 1990).

ERA	PERIOD	EPOCH	FORMATION	DESCRIPTION	
CENOZOIC	QUATERNARY	HOLOCENE	ALLUVIUM	Sandstone, clay, shale and conglomerate	
		PLIOCENE-PLEISTOCENE	SIWALIK	Sandstone, shale and conglomerate	
	TERTIARY	MIOCENE	GAJ	Shale, sandstone and limestone	
		OLIGOCENE	NARI	Shale, limestone and sandstone	
		EOCENE	LATE		
			MIDDLE	KIRTHAR	Limestone and shale
			EARLY	LAKI/GHAZIJI	Laki: Limestone and shale Ghazi: Shale and sandstone
		PALEOCENE	BARA-LAKHRA	Limestone, shale and sandstone	
	KHADRO		Basalt and Shale		
	MESOZOIC	CRETACEOUS	LATE	PAB	Sandstone and Shale
MUGHAL KOT				Limestone, shale and minor sand	
PARH				Limestone	
MIDDLE			GORU	UPPER	MAIN SEAL Shale and marl
				LOWER	Shale and sandstone
				SEMBAR	MAIN SOURCE Shale and sandstone
EARLY					
JURASSIC		LATE			
		MIDDLE	MAZAR DRIK	Limestone	
			CHILTAN	Limestone and shale	
EARLY	SHIRINAB	Limestone, shale and sandstone			
TRIASSIC		EARLY-LATE	WULGAI	Shale and sandstone	

**Figure 2. 3** Generalized stratigraphic sequence in the Lower Indus Basin (modified after Shah, 1977; Raza et al., 1990).

## **CHAPTER 3**

### **MATERIAL AND METHODOLOGY**

#### **3.1 Wells Selection**

Two wells were selected from the Jabo field of Badin Block (figure 3.1) of the Lower Indus Basin for petrophysical analysis.

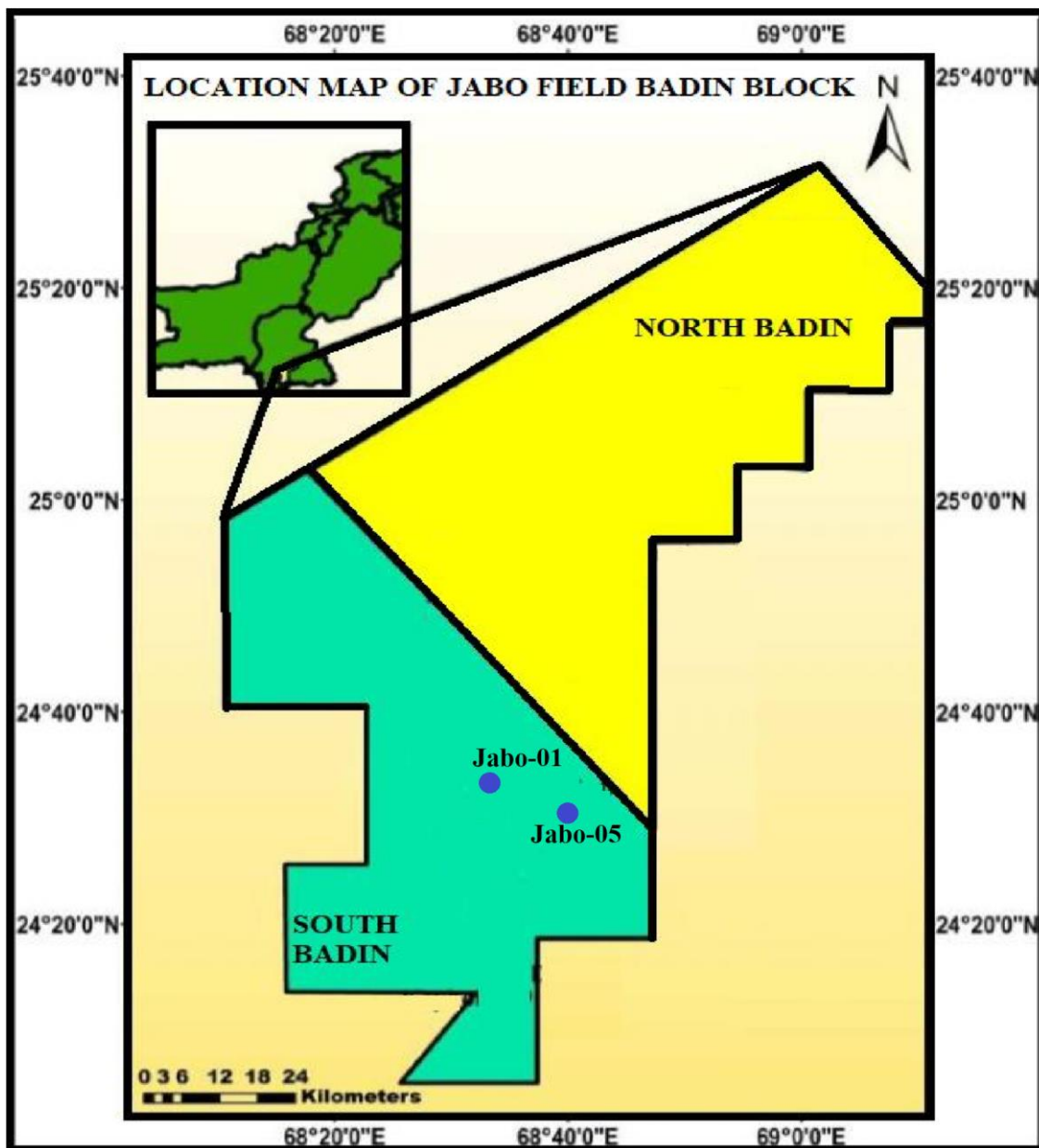


**Figure 3.1** Generated map showing the location of the Jabo field of the Badin Block.

### 3.2 Jabo-01:

It is an exploratory well for the Jabo concession having latitude 24°21'31.13" and longitude 68°33'16.20". Union Texas Pakistan was the operator of the well. The Spud date for this well was 15 May 1986 that completed on 15 June 1986 which ultimately produced gas and condensates initially while later on it was abandoned. The total depth for this well is 2229 m ending in the Lower Goru Formation which is acting as a reservoir of the well. Lithology encountered in the well is given in table 3.1.

**Table 3.1** Formation tops and thicknesses in Jabo-01

Formations Name	Age	Tops (m)	Thickness(m)
Alluvium	Recent	0	5.5
Gaj-Nari	Oligocene to Miocene	5.5	94.5
Kirthar and Laki Shale	Paleocene-Eocene	100	302
Lower Ranikot	Paleocene	402	206
Khadro (Basalt)	Early Paleocene	608	51
Parh Limestone	Late Cretaceous	659	40.5
Upper Goru	Late Cretaceous	699.5	1278.5
Lower Goru	Early Cretaceous	1978.75	250
TD (Total Depth)		2229	

### 3.3 JAB0-05

It is a development well and operated by BP (British Petroleum) for further development of the Jabo field. It is located at 24°21'8.49" and longitude 68°33'16.00". Jabo-05 is relatively shallower than the first well with a total depth of 2075.60m. The same reservoir produced oil and gas both from this well. Formation tops along with thicknesses are mentioned in table 3.2.

**Table 3.2** Formation tops and thicknesses in Jabo-05

Zone Name	Age	Top depth (m)	Thickness (m)
Alluvium	Recent	0	79
Gaj-Nari	Oligocene- Miocene	79	144.77
Upper Ranikot	Paleocene	350.50	274.31
Khadro Basalt	Paleocene	624.81	41.15
Parh Limestone	Late Cretaceous	665.96	27.43
Upper Goru	Late Cretaceous	693.39	1245.04
Lower Goru	Early Cretaceous	1938.43	94
B Sand	Early Cretaceous	1950.63	54.86
Badin Shale	Early Cretaceous	2005.49	27.43
Sand Below Badin Shale	Early Cretaceous	2032.92	43.08
TD (total Depth)		2076	

### 3.4 Petrophysical Analysis

Petrophysics was first introduced by G.E. ('GUS') Archie in the late 1940s as the study of the physics of rocks (Kennedy, 2015). The petrophysics tells about the relationship of rocks with fluids in the subsurface by using different logging tools (e.g., Kumar et al., 2017). The different logs used for interpretation in this research are referred in table 3.3.

**Table 3.3** Well logs used for petrophysical interpretation

<b>Lithological Logs</b>	<b>Porosity Logs</b>	<b>Fluid Dynamics</b>	<b>Bore Hole Size</b>
Gamma Ray Log(GR)	Sonic Log	Resistivity logs(MSFL,LLS&LLD)	Caliper Log
Self -Potential Log (SP)	Neutron Log (NPHIE)		
	Density Log (RHOB)		

Petrophysical analysis by these logs and petrophysical properties calculated, which were used to identify reservoir characterization, later on, are listed below.

- 1) Lithology
- 2) Washout
- 3) Density
- 4) Porosity
- 5) Formation temperature
- 6) Volume of shale
- 7) Water saturation
- 8) Hydrocarbon saturation

### 3.5 Quality Check

The data obtained from LMKR by the approval of DGPC was checked thoroughly to confirm the suitability of the data for petrophysical analysis. LAS files were loaded in the Geographix software and were checked that the required logs were run in the reservoir zone or not and compatibility of logs.

### **3.6 Selection of Zones**

The zone of interest was selected by observing log trends for the reservoir. Criteria used for the zone selection are as follow:

1. GR log trend indicating clean zones
2. High resistivity values which are an indication of hydrocarbon presence
3. The caliper log trend was observed to find out any bad hole conditions.
4. Good porosity zones were calculated from sonic, density, and neutron logs.

### **3.7 Reservoir Evaluation**

Petrophysical evaluation involves the following measurements to evaluate reservoir parameters.

#### **3.7.1 Volume of Shale**

GR log was used for the measurement of the volume of shale. Higher GR values (on the log scale) indicate the presence of shale/dirty facies because of the higher amount of radioactive minerals present as compared to sandstone and limestone. The scale used for GR log ranges from 0 to 150 API. The volume of shale is measures by placing the shale baseline (highest most value on GR curve as per the log scale) and sand baseline by observing log trend on the lowest most curve reading on the scale. Equation (Schlumberger, 1974) used for measuring the volume shale/dirty facies is following



$$\text{IGR} = V_{\text{sh}} = (\text{GR}_{\text{log}} - \text{GR}_{\text{min}}) \div (\text{GR}_{\text{max}} - \text{GR}_{\text{min}})$$

Where,

IGR = Gamma-Ray Index

V<sub>sh</sub> = Volume of Shale/dirty facies

GR<sub>log</sub> = Gamma-Ray value at the desired depth

GR<sub>min</sub> = Minimum GR reading

GR<sub>max</sub> = Maximum GR reading

The volume of clean lithology can be calculated by using the following equation (Schlumberger, 1974).

$$V_{\text{clean}} = 1 - V_{\text{sh}}$$

$$V_{\text{sh}} = 1 - V_{\text{clean}}$$

V<sub>clean</sub> = Volume of clean zone

### 3.7.2 Porosity Measurement

There are different methods for porosity calculation that are used respective to their limitations.

#### 3.7.2.1 Density Porosity (DPHI)

The density porosity is calculated from the density log. The principle of density log is to measure the bulk density by detecting the number of gamma rays emitted by a source on the detector. The following equation is used for the calculation of porosity (Schlumberger, 1989).

$$\Phi = (\rho_{\text{ma}} - \rho_{\text{b}}) \div (\rho_{\text{ma}} - \rho_{\text{f}})$$

Where,

$\Phi$  = Density porosity

$\rho_{ma}$  = Density of matrix.

$\rho_b$  = Bulk density of the formation  $\rho$

$\rho_f$  = Density of fluid (Saline Water = 1.1 gm/cm<sup>3</sup>)

The density tool is a padded/contact tool that remains in contact with the borehole while measurement. The logging tool emits gamma-ray which collides with electrons of the formation and scatter. The detector on the tool measures the returning gamma rays which are an indicator of the bulk density of the formation.

Density is not reliable in bad hole conditions (washouts) because it is a padded tool and it will measure the bulk density of mud instead of formation. Matrix density for sandstone is 2.65 g/cc, limestone 2.71, and 2.876 for dolomite.

### 3.7.2.2 Neutron Porosity (NPHI)

Neutron porosity is measured with the help of a neutron log. Neutron log measures the hydrogen concentration in a formation. It is a noncontact tool that bombards neutrons from a source that collides with the nuclei of the formation and loses some energy. Maximum energy loss occurs on collision with hydrogen atoms because of the similar size of the neutron as hydrogen atoms.

Neutron energy loss is related to porosity because, in porous formations, hydrogen is concentrated in the fluid filling the pores. Lithology, porosity, and fluid type affect neutron log response. It indicates lower porosity for gas-filled pores as compared to oil and water-filled pores because of lower hydrogen concentration. The advantage of a neutron log is that it can also measure in a cased hole.

### 3.7.2.3 Sonic Porosity

This is determined by the sonic log which measures the travel time of waves from the source to the detector. The range of scale for the sonic log is 40-240  $\mu\text{s}/\text{ft}$ . The equation used for determining the sonic porosity is given below.

$$S_{\text{phi}} = (\Delta_t - \Delta_{\text{tma}}) \div (\Delta_{\text{tf}} - \Delta_{\text{tma}})$$

Where,

$S_{\text{phi}}$  = Sonic porosity

$\Delta_t$  = Travel time from sonic log

$\Delta_{\text{tma}}$  = Travel time information through its matrix

$\Delta_{\text{tf}}$  = Travel time in the fluid present in the formation.

### 3.7.2.4 Average ( $A_{\text{PHI}}$ ) and Effective Porosity ( $E_{\text{PHI}}$ )

Average porosity is determined by averaging the values of average neutron porosity values throughout the reservoir zone and average density porosity throughout the reservoir zone. The equation used for the determination of average neutron-Density porosity is as follows (Serra, 1984).

$$A_{\text{PHI}} = \{(N_{\text{PHI}}) + (D_{\text{PHI}})\} \div 2$$

If caving/bad hole conditions are absent as per the caliper log curve signatures in comparison with borehole size, the effective porosity will be calculated from the equation-i (Serra, 1984), and in the case of caving/bad hole, the equation-ii based on sonic porosity can be used.

$$E_{\text{PHI}} = (A_{\text{PHI}}) \times (V_{\text{clean}}) \text{ ----- Eq (i)}$$

$$(E_{\text{PHI}}) = (S_{\text{PHI}}) \times (V_{\text{clean}}) \text{ ----- Eq (ii)}$$

### 3.7.3 Spontaneous Potential

SP log measures the potential difference between the moveable electrode in the borehole and the electrode on the surface. When borehole fluids get in contact with formation fluids, an electric potential is generated known as a liquid junction along with the permeable layer. Shale gets negatively charged when Na<sup>+</sup> ions pass through it to less saline water (borehole fluid), a potential development which is known as the membrane potential.

$$E_{\text{total}} = E_{\text{lj}} + E_{\text{m}}$$

Where,

$E_{\text{total}}$  is total SP potential.

$E_{\text{lj}}$  is the potential of the liquid junction.

$E_{\text{m}}$  is potential of membrane potential.

SP log is measured in millivolts. It cannot read in conductive muds or offshore. SP is used to identify permeable beds, the environment of deposition, and the calculation of  $R_w$  (resistivity of formation water). Analysis using the law of physical chemistry leads to equation:

$$SP = -K [\log (R_{\text{mf}}/R_w)]$$

Where,

$K$  = constant (depends on temperature)

$R_{\text{mf}}$  = resistivity of mud filtrate

$R_w$  = resistivity of water

$K$  can be estimated from the temperature of formation for sands from the equation:

$$K = (T_f + 505)/8$$

Where  $T_f$  is formation temperature in Fahrenheit, and Degree Celsius from the equation:

$$K = (T_f + 336)/5$$

### 3.7.4 Resistivity of Water ( $R_w$ )

The water resistivity of formation is determined by using a set of equations stated below.

$$\text{Geothermal Gradient} = G.G$$

$$G.G = (\text{Borehole Temperature} - \text{Surface Temperature}) \div \text{Total Depth}$$

$$\text{Formation Temperature} = (\text{Formation Top} \times G.G) + \text{Surface Temperature}$$

After calculation, the conversion of  $R_{mf}$  at surface temperature to  $R_{mf}$  at formation temperature will be done with help of the GEN-9, SP-1, and SP-2 charts (figure 3.2, 3.3, and 3.4). Note that if  $R_{mf} > 0.1$ ,  $R_{mf \text{ eq}} = R_{mf} \times 0.85$ . After this, the conversion of  $R_{mf}$  to  $R_{mf \text{ eq}}$  will be done with help of the SP-2 chart. Now with help of the Self Potential (SP) log highest and lowest curve reading will be selected and added to it. After this with help of the SP-1 chart,  $R_{w \text{ eq}}$  will be determined. In the end, the conversion of  $R_{w \text{ eq}}$  to  $R_w$  will be carried out using the SP-2 chart.

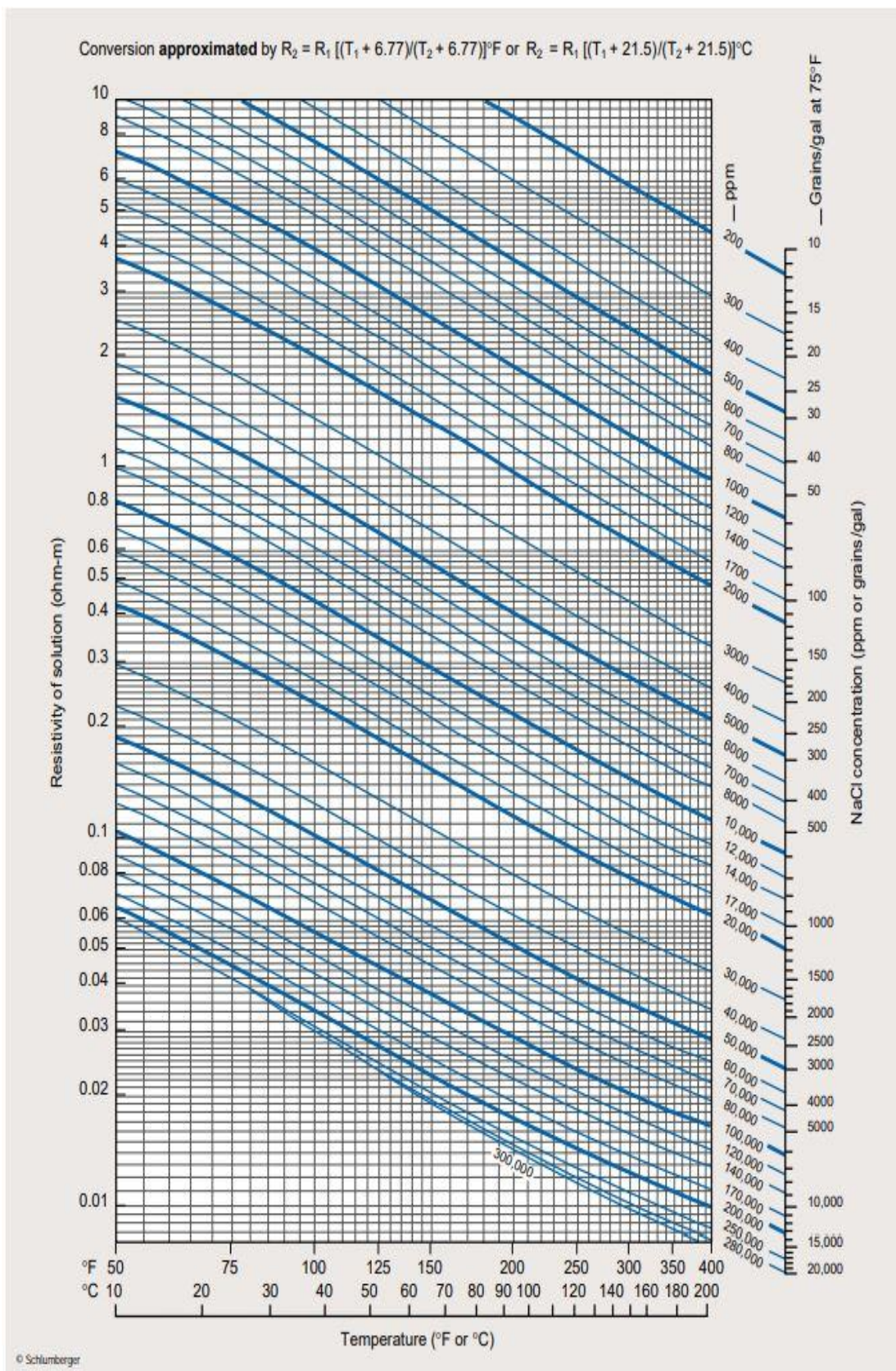


Figure 3.2 Schlumberger Gen-9 chart.

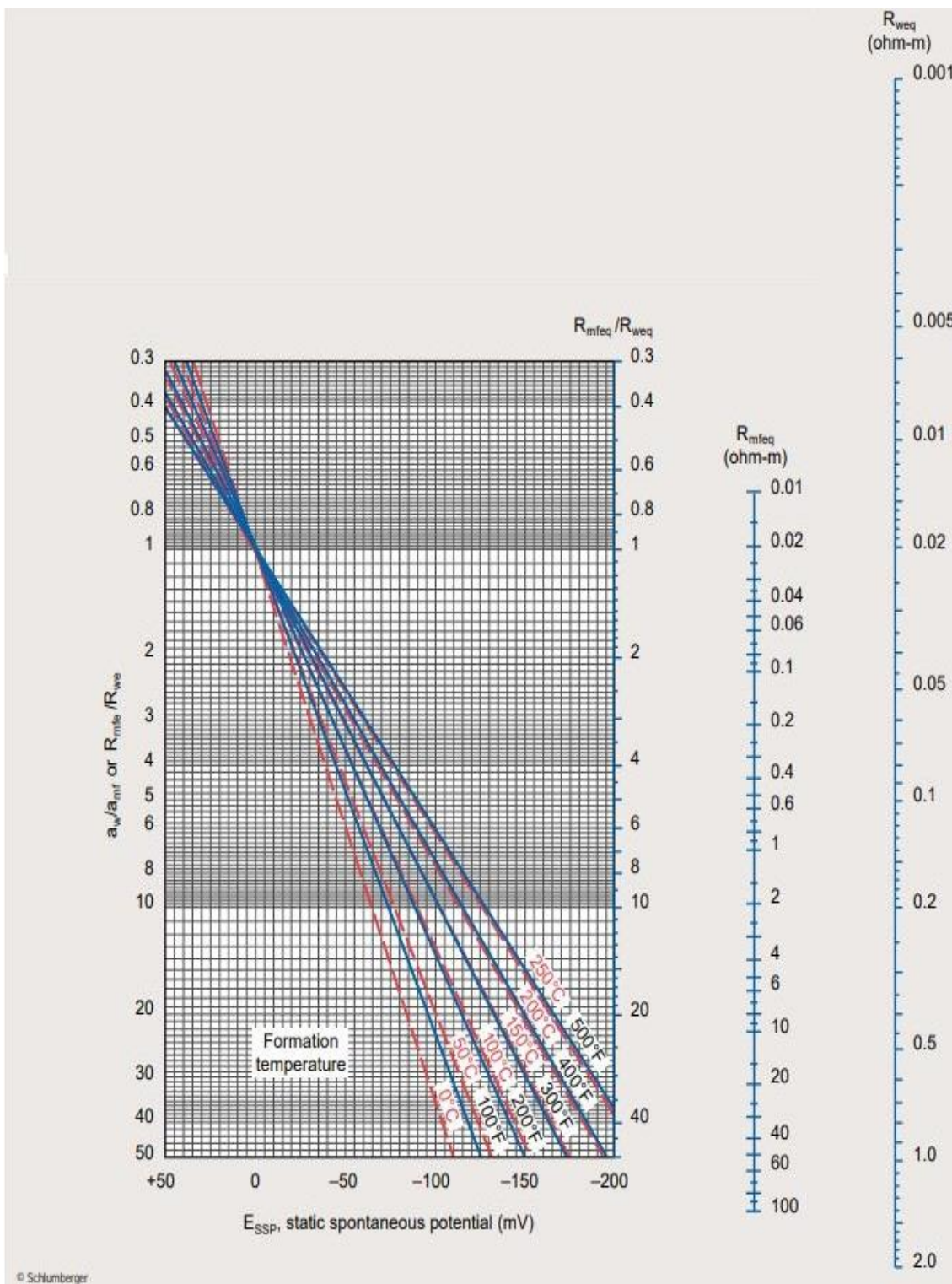
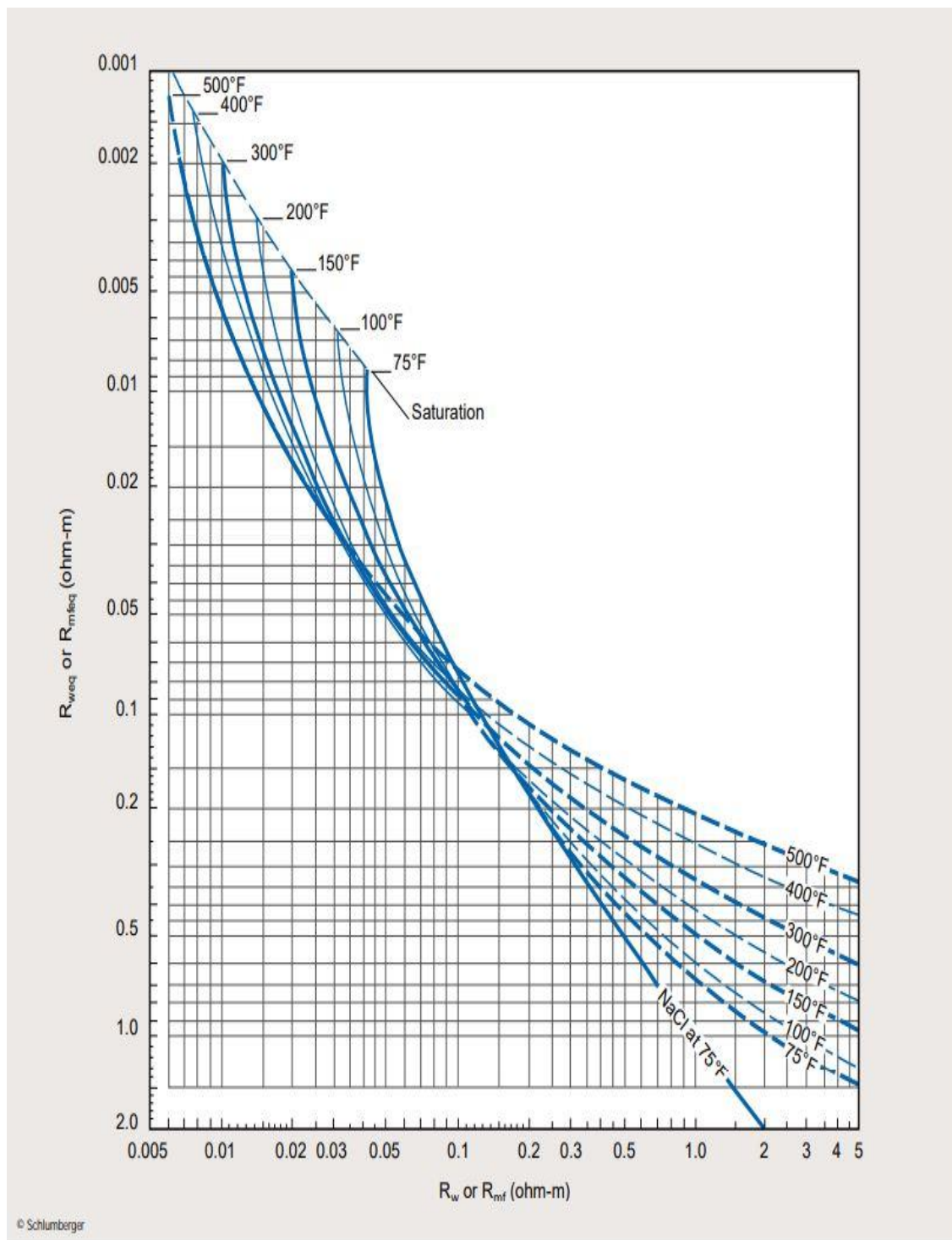


Figure 3.3 Schlumberger SP-1 chart.



**Figure 3.4** Schlumberger SP-2 chart.



### 3.7.5 Water Saturation ( $S_w$ ) and Hydrocarbon Saturation ( $S_h$ )

$S_w$  is the amount of water filled in pore spaces of rock while  $S_h$  is the amount of hydrocarbon in the pore spaces of the rock. Archie equation will be applied for water saturation calculation

$$S_w = [(a \div \Phi^m) \times (R_w / R_t)]^{1/n}$$

Where,

a= Tortuosity factor

$\Phi$ = Porosity

m= Cementation component

n= Saturation component

The following equation will be used to calculate hydrocarbon saturation.

$$S_h = 1 - S_w$$

### 3.8 Seismic Data

Eight 2-D seismic lines were selected for structural interpretation which is given (Table 3.4).

**Table 3. 4** List of seismic lines used for interpretation.

S. No	Lines Names	Lines Nature
1	PK85-KH-01	Strike Line
2	PK85-KH-04	Dip Line
3	PK85-KH-06	Dip Line
4	PK85-0958	Dip Line
5	PK85-0937	Strike Line
6	PK86-1200	Dip Line
7	PK86-1202	Dip Line
8	PK92-1678	Dip Line

### 3.9 Data Quality Check

Seismic data obtained was loaded and checked to confirm its navigation and grid. One of the wells (Jabo-01) lies exactly on the seismic line as well location on line gives good control for interpretation. QC of data revealed that the provided data was suitable enough to carry out seismic interpretation.

### 3.10 Base Map

Seismic lines grid and wells location were loaded on kingdom software to generate the base map. The base map (figure 3.2) shows well Jabo-01 is on seismic line GPK86-1200 (dip line) which was used as a control line for the seismic interpretation.

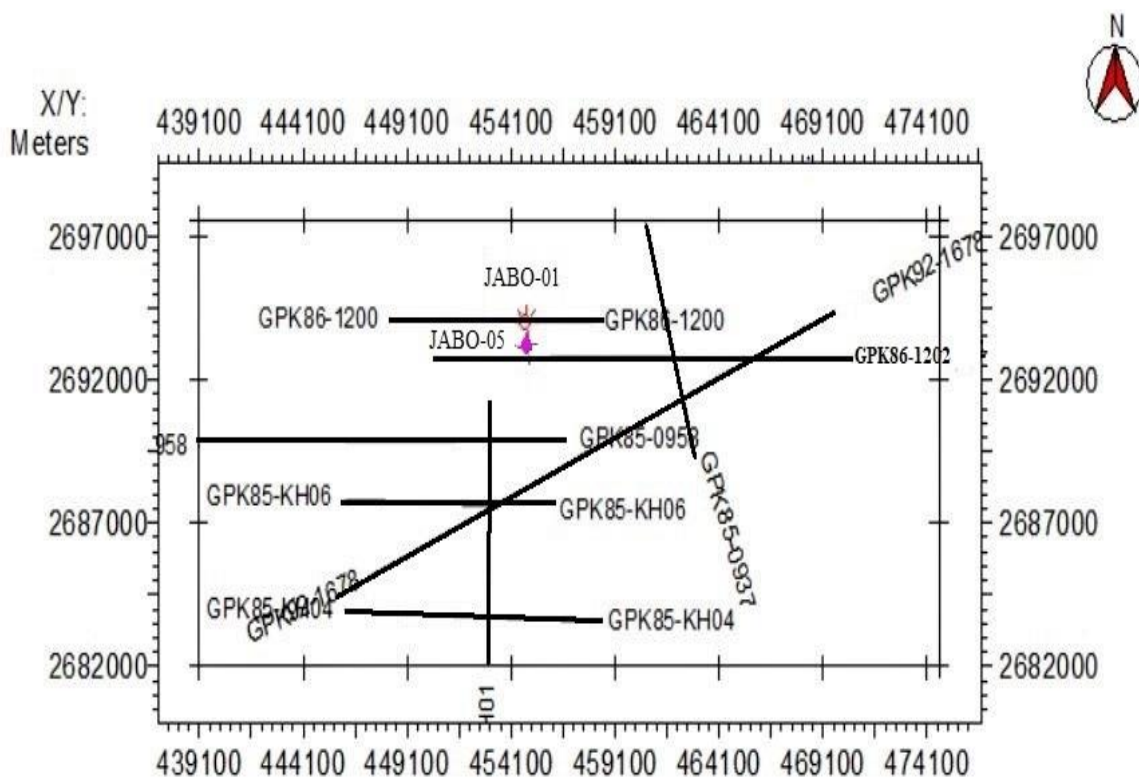


**Figure 3.5** Base map of selected seismic lines.

### **3.11 Seismic Approaches**

Seismic data can be interpreted by using two principal approaches:

- 1) Structural Interpretation
- 2) Stratigraphic Interpretation

#### **3.11.1 Structural Interpretation:**

The main objective of structural interpretation is to identify the existence of the structural traps, anticlines, folds, and faults. By identifying potential structures in the subsurface which are capable of accumulating hydrocarbons it is then decided to consider the area for further investigation.

#### **3.11.2 Stratigraphic Interpretation**

Stratigraphic analysis of seismic sections is the identification of different Formations which are known as horizons in geophysical sciences. The stratigraphic interpretation of seismic lines was done by marking horizons with help of well data.

### **3.12 Well to Seismic Tie**

It is a principle step in seismic understanding in which seismic sections and wells are correlated. Data acquired from the wellbore is in-depth and in the seismic survey, the acquired information is in time. Time and depth relation is built to mark horizons.

### **3.13 Synthetic Seismogram**

The purpose of a synthetic seismogram is to confirm the selected horizons. GR, DT, and RHOB logs are used to generate synthetic seismograms. Velocities are obtained from DT and RHOB log. Besides, this GR log is used as a reference log.

### **3.14 Contour Maps**

Contour maps were generated for two horizons tops (Lower Goru and Upper Goru) with time as well as depth to predict the dipping trend.

## **Chapter 4**

### **Petrophysical Interpretation**

#### **4.1 Jabo 01**

GR log in figure 4.1, from 1980 meters to 1995 meters there is a serrated trend which indicates shoreface deposits. From 1995 to 2010, there is a cylindrical trend showing barrier bar and beach bar deposition and for 2010 to 2025 meters is again serrated trend indicating transgressive marine deposition. Below 2025 meters GR curve forms cylindrical trend confirming submarine shallow marine shelf deposits.

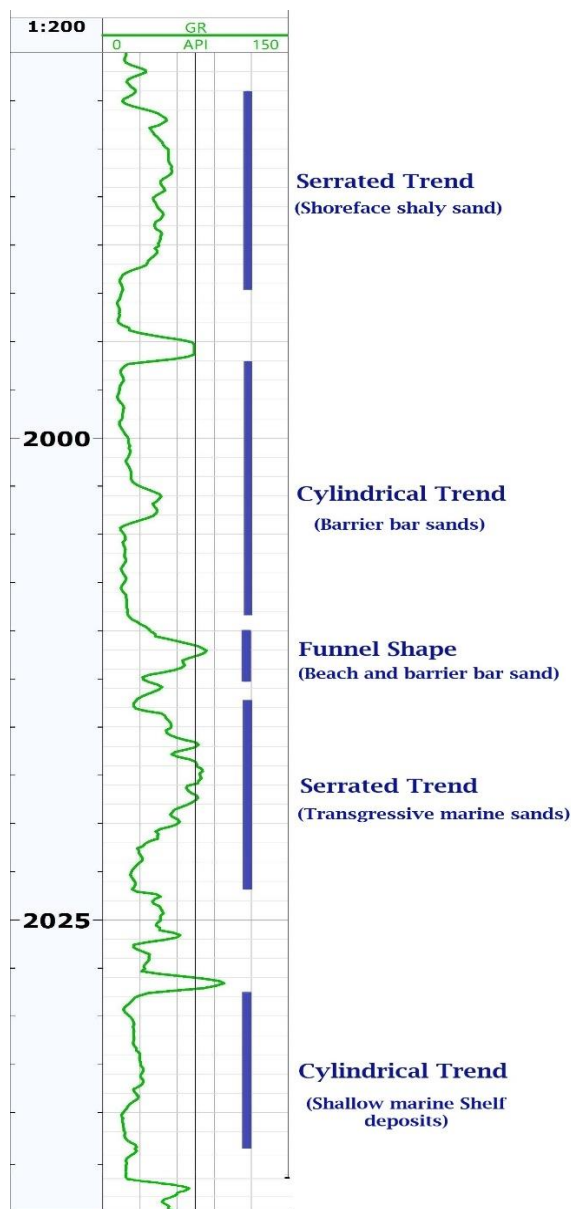


**Figure 4.1** Environment of deposition of Lower Goru Formation in Jabo-01 well.

For petrophysical analysis whole log suite was observed, the zone of interest was identified and selected for interpretation (figure 4.2). Gamma-ray log was used to locate sand and shale zones. Clean zones were marked following the GR log trend (figure 4.2).

Bad hole conditions can be observed by the curve signature of caliper log (figure 4.2) which ultimately makes the log readings of RHOB and NPHI problematic, hence sonic porosity was used for porosity measurement in well Jabo-01.

GR log was used for the calculation of the volume of shale. Noticeable deflections between MSFL, LLS, and LLD curves along with PHIE and  $S_w$  curves behavior is an indication of possible hydrocarbons.

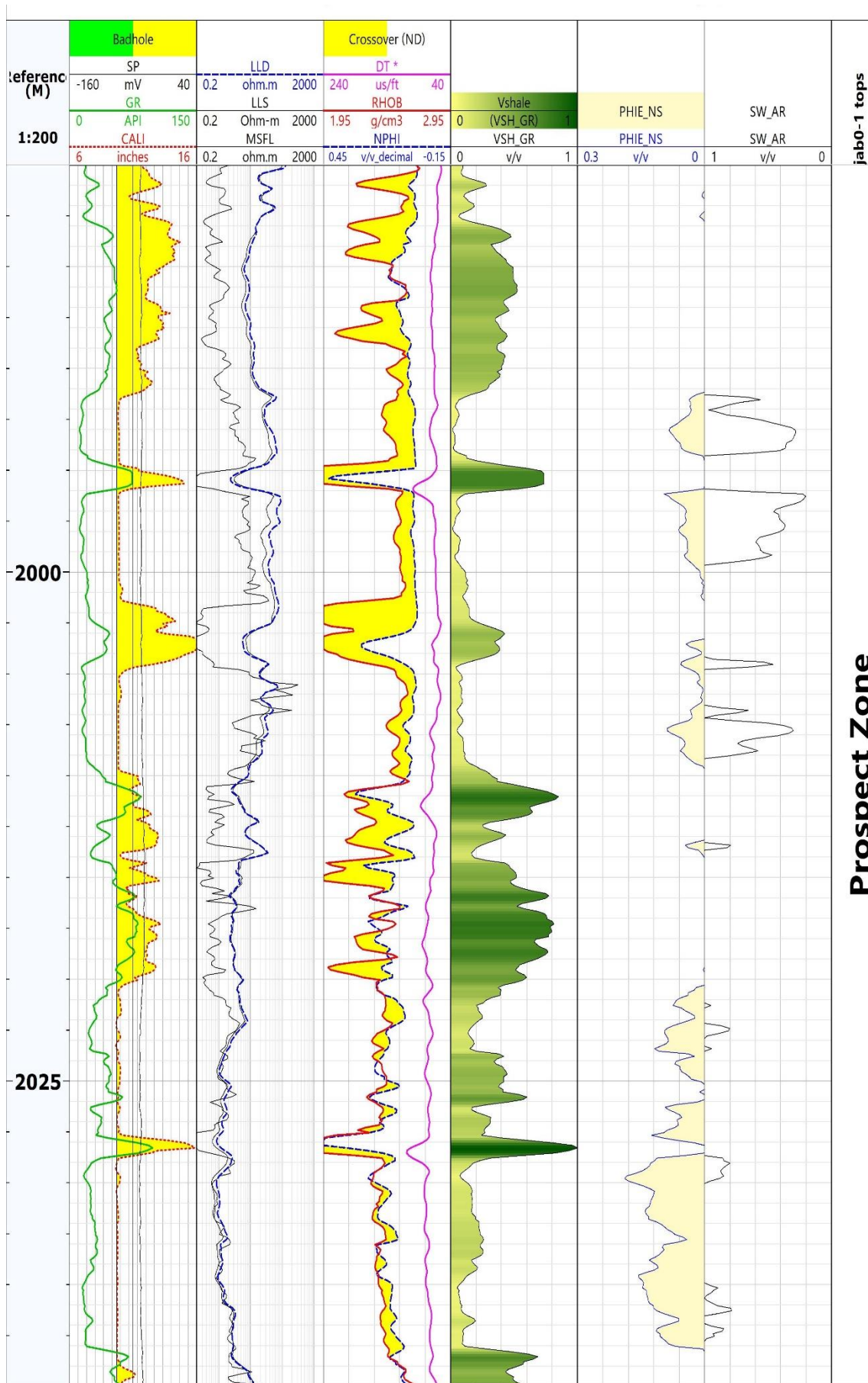


Figure 4.2 Petrophysical interpretation of Lower Goru Formation in Jabo-01



The following table shows the reservoir summary calculated from the given well data and equations for the pay zone.

**Table 4.1** Reservoir summary for Jabo-01

<b>Well</b>	<b>Jabo-01</b>
Gross Thickness	60 m
Net	12 m
Net to Gross	0.2
Average volume of shale	19.8%
Average effective porosity	8.2%
Average water saturation	78.8%
Average hydrocarbon saturation	21.2%

## 4.2 Jabo 05

GR log was used to find out the environment of deposition of the Lower Goru Formation. It can be seen in figure 4.3, there is a serrated trend indicating shoreface deposition above 1955 meters. The section ranging from 1955 meters to 1975 meters is barrier and beach bar deposit as GR signatures cylindrical trend. There is a serrated trend confirming an episode of transgressive marine deposition from 1980 meters to 1990 meters and shallow marine shelf deposit ranges were observed below 1995 meters.

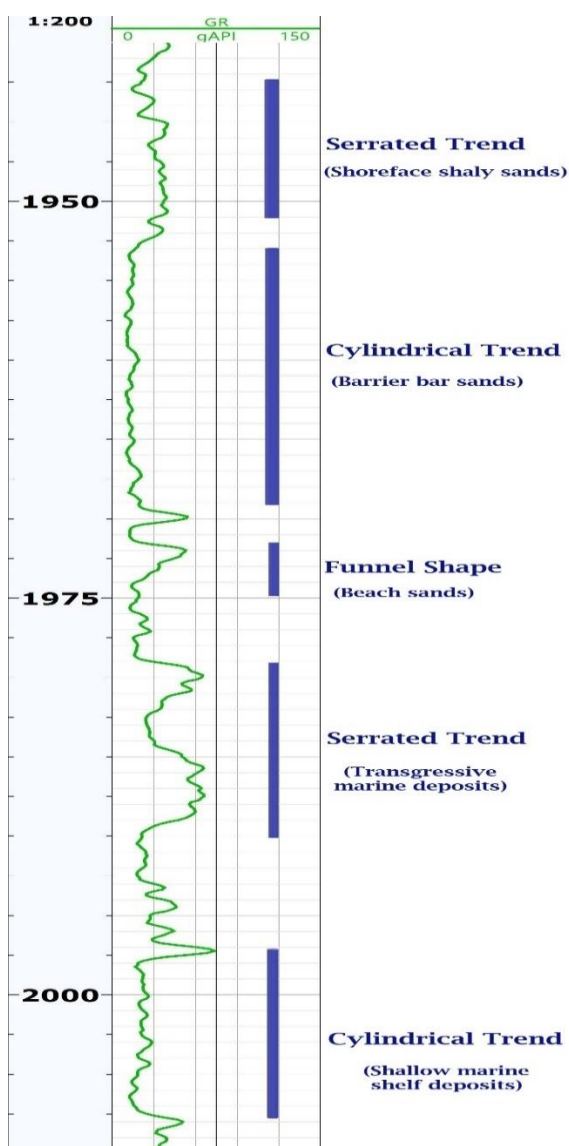


**Figure 4.3** Environment of deposition of Lower Goru Formation in Jabo-05 well.

To begin with, clean zones were marked by the following GR curves (figure 4.4). Borehole conditions were good for Jabo-05, the caliper log was steady indicating the absence of washouts which validates RHOB and NPHIE values, so they were used for the porosity calculations.

The volume of shale was calculated by marking sand and shale baselines along the GR log curves precisely. The saturation of water was calculated by using Archie's equation.

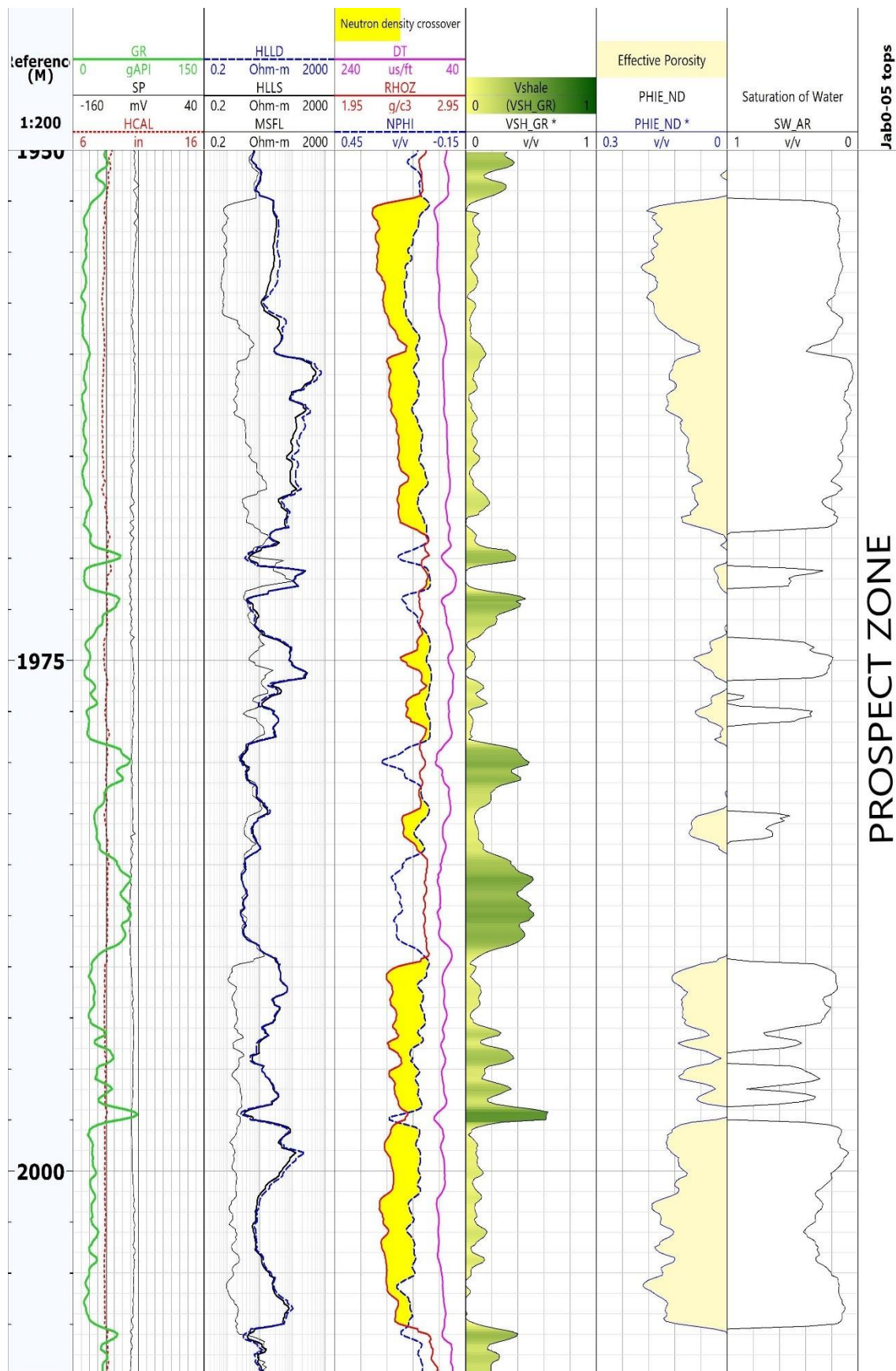


Figure 4.4 Petrophysical interpretation of Lower Goru Formation in Jabo-05

The following table shows the reservoir summary calculated from the given well data and equations for the clean zone.

**Table 4.2** Reservoir summary for Jabo-05.

<b>Well</b>	<b>Jabo-05</b>
Flag Name	Pay
Gross Thickness	60
Net	37.9
Net to Gross	0.63
The average volume of shale	17%
Average effective porosity	7.15%
Average water saturation	45.24%
Average hydrocarbon saturation	54.76%

### 4.3 Correlation

The petrophysical comparison of both wells is shown in figure 4.5. The Lower Goru Formation was encountered at various depths in both wells. It was experienced at a greater depth in the Jabo-01 in comparison with Jabo-05. About 25 meters difference in depth of the reservoir is a direct result of horst and graben structures in the region can be observed along with normal faults in interpreted seismic lines (figure 5.4, 5.6, 5.7, 5.9, and 5.10).

Despite the depth, excellent comparable log trends can be observed in both wells which indicates the presence of similar lithology. Effective porosity in Jabo-01 is lower than Jabo-05 due to washouts in Jabo-01. It can be observed from the GR log trend that sandstone is abundant in both wells. The volume of shale is lower in the Jabo-05 which shows a gradual increase in reservoir quality in the southward direction of the field.

Saturations of Jabo-01 well indicates that the reservoir of this well is more water-wet and having hydrocarbon saturations below 20% while Jabo-05 is more hydrocarbon-rich which is about 41%. It also indicates that saturations trend are better in the southern part of the field.

**Table 4.3** Reservoir summary comparison

Well	Jabo-01	Jabo-05
Flag Name	Pay	Pay
Gross Thickness	60 m	60 m
Net	12 m	37.9 m
Net to Gross	0.2	0.63
Average volume of shale	19.8%	17%
Average porosity	8.2%	7.15%
Average water saturation	78.8%	45.24%
Average hydrocarbon saturation	21.2%	54.76%

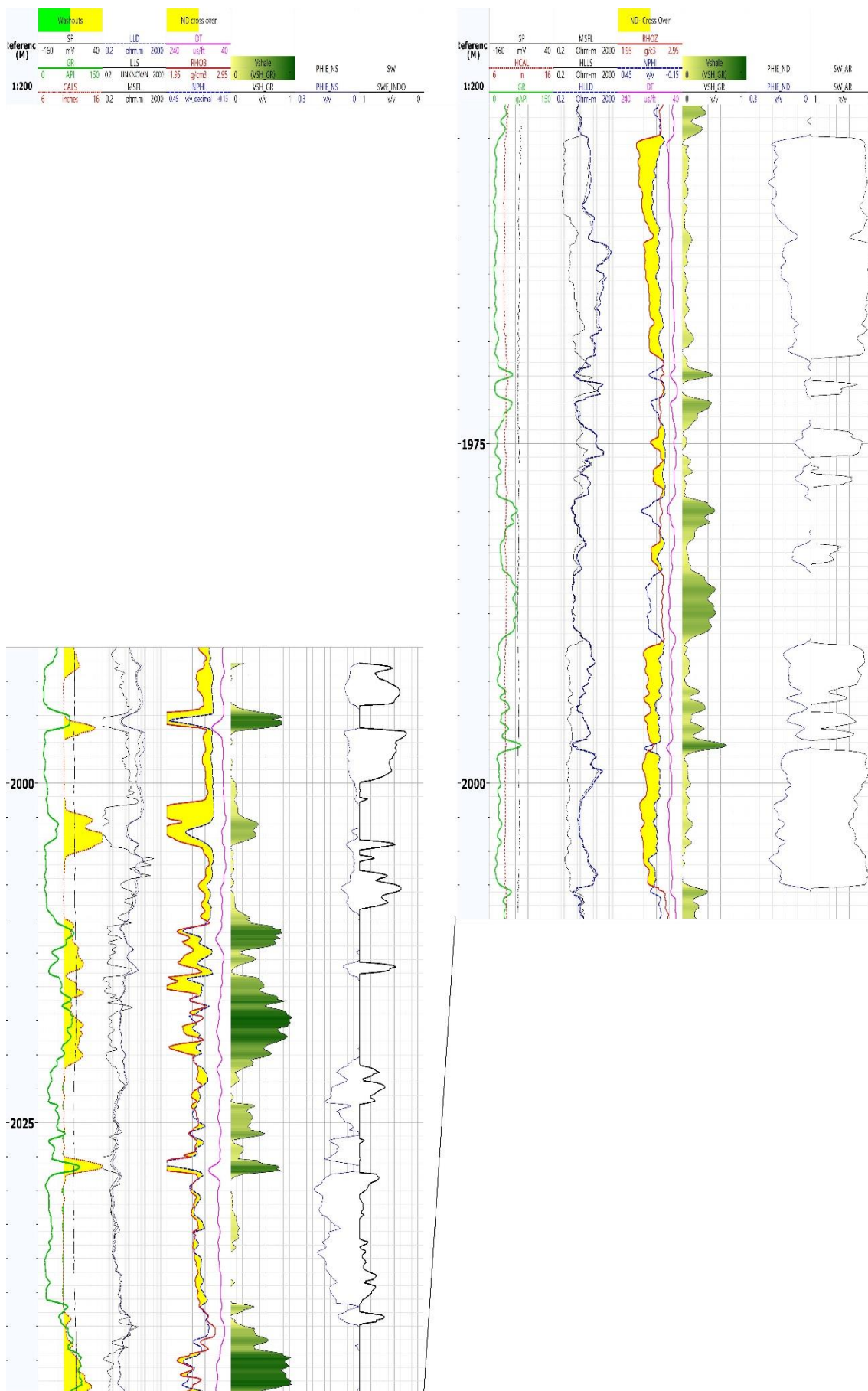
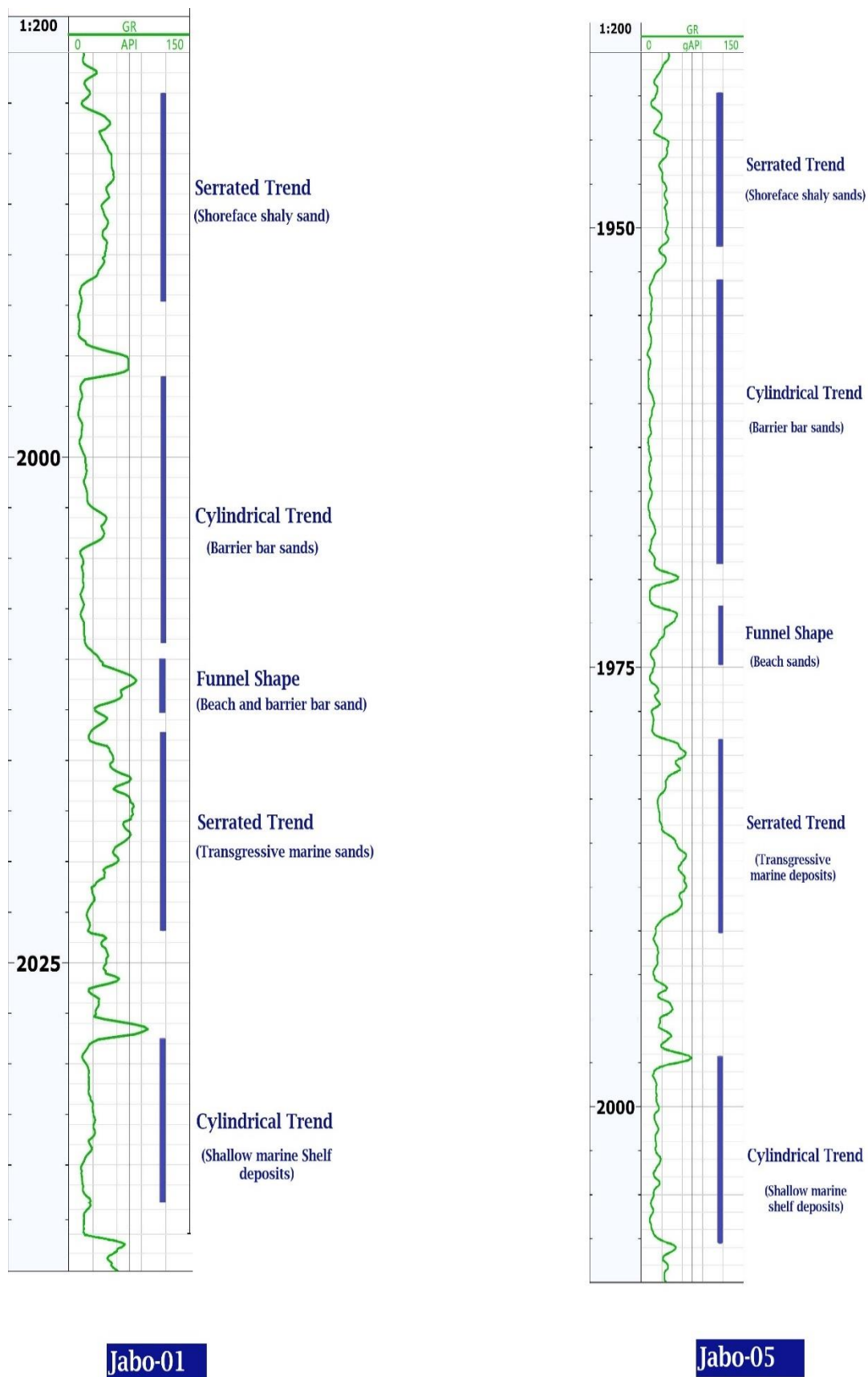


Figure 4.5 Correlation of Lower Goru Formation in Jabo-01 and Jabo-05



**Figure 4.6** Correlation of environment of deposition of Lower Goru Formation in Jabo-01 and Jabo-05.



## 4.4 Lithological Identification

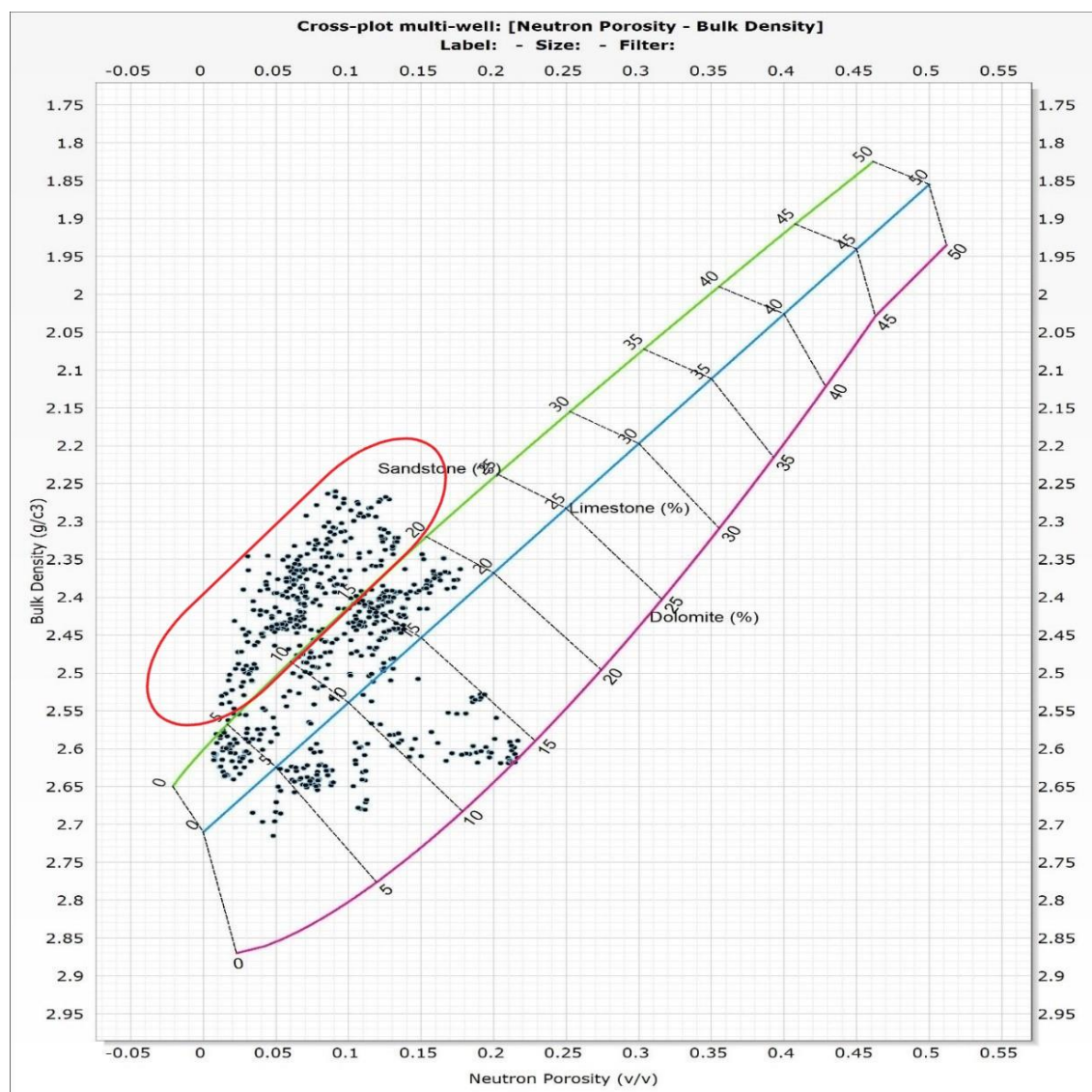


**Figure 4.7** Cross plot between neutron and density for lithological identification.

Neutron and density log calculations were used to develop a cross plot (figure 4.7.) for Jabo-05 well as due to bad hole conditions of Jabo-01 made these log readings problematic. Schlumberger CP-1c and CP-1D, neutron vs bulk density chart was used to generate the cross plot. It was observed from the results that the majority of values fall adjacent to the sandstone boundary which confirms the abundance of sandstone in the interpreted zone, marked sands are the producing sands of Jabo-05. In addition to this low GR values also confirm the abundance of sandstone.

The Cross plot also indicates the presence of carbonates in the reservoir. Scattered points are because of washouts and shales. Lower density values are due to the presence of heavy minerals in it which require a mud log for complete interpretation.

#### **4.4.1 Lithological Identification from Rock Physics**

Rock physics is a very important technique that links geological and geophysical parameters used for reservoir characterization (Golyan, 2012). Reservoir characterization is used widely to lower the risk of hydrocarbon exploration failures. Pore fluids and lithological identification are very important in reservoir characterization. Characterization of the mature reservoir may require unconventional tools (Golyan, 2012).

The cross plots are the visual representation to detect and identify anomalies in hydrocarbon, lithology, and other fluids present in the formations (Omudu et al., 2007).

The following cross plots are used in this research to discriminate lithology.

1. Acoustic impedance and  $V_p/V_s$  ratio
2. Mu-rho and density
3. Incompressibility and  $V_p/V_s$

##### **4.4.1.1 Acoustic Impedance and $V_p/V_s$**

$V_p$  is the p-wave velocity and  $V_s$  is the s-wave velocity calculated from the sonic log (DT). The cross plot of the p-impedance vs  $V_p$  and  $V_s$  ratio is shown in figure 4.8.

$V_p/V_s$  ratio ranges from 1.68 to 1.8 for gas sands and above 1.8 are considered as brine sand while the value of p-impedance for hydrocarbons is very low (Das and Chatterjee, 2018).

By using these ranges gas sands are circled (figure 4.8). The low value of p-impedance is indicating hydrocarbons. This cross plot was developed with reference to effective porosity where purple color is indicating shales and while blue, green, and yellow color is indicating brine sands. The range of  $V_p/V_s$  ratio in figure 4.8 is from 1.7 to 1.8 for gas sands are marked.

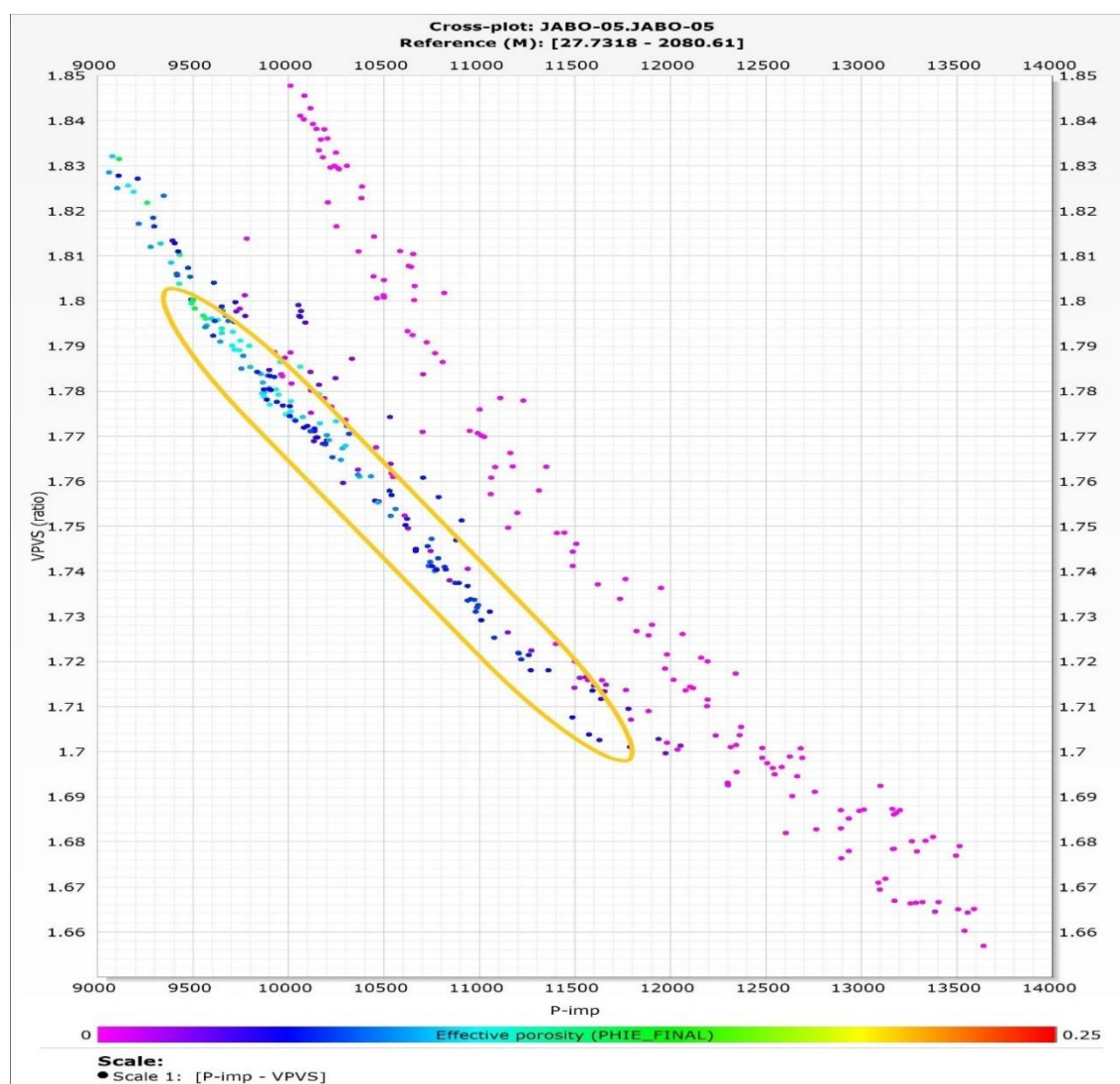


**Figure 4.8** Cross plot between P-imp and  $V_p/V_s$  ratio for well Jabo-05 and effective porosity is shown in the color legend.

#### 4.4.1.2 Mu-Rho and Density

The cross plot of Mu-Rho (rigidity) and density is generated for the prospect zone shown in figure (4.9). The value of Mu-Rho for gas sands will be higher than 15 GPa and density values will be lower for gas. Intermediate values indicate brine sand (Das and Chaterjee, (2018)). Points within the eclipse are gas sands, purple points are showing gas sands while the rest of the points are indicating brine sands (figure 4.9). Effective porosity was used as a color reference as one can infer that effective porosity for shales is almost zero.

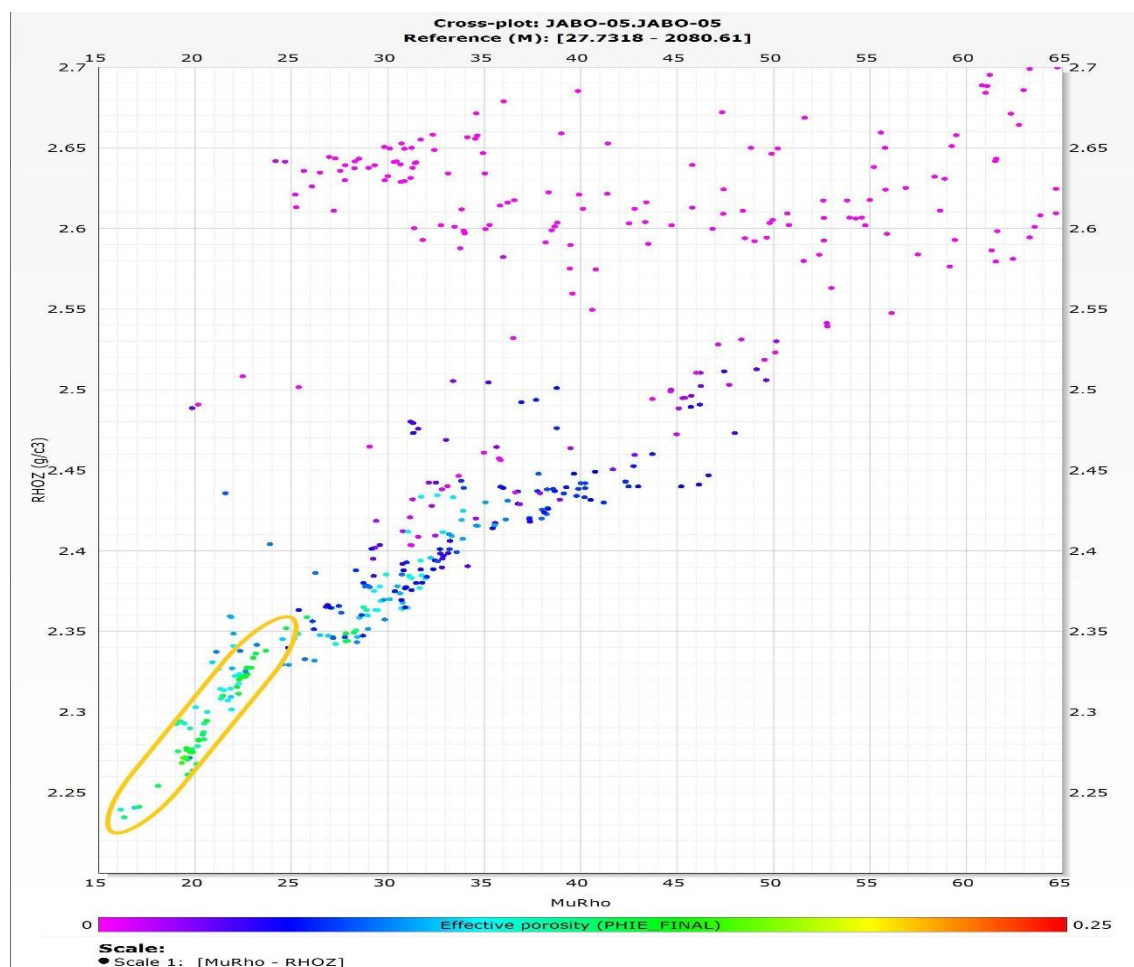


**Figure 4.9** Cross plot between density and MuRho for well Jabo-05 and gamma ray is shown in the color legend.

#### 4.4.1.3 Incompressibility and Mu-Rho

The lambda-rho is incompressibility and Mu-rho is rigidity. The values of lambda-rho higher than 20 GPa and values of Mu-rho higher than 15 GPa approximately indicate gas sands (Das and Chaterjee, 2018). The cross plot of lambda-rho ( $\lambda\rho$ ) vs. mu-rho ( $\mu\rho$ ) discriminate brine zone (blue dots) and shale zones (purple points) while green points indicate gas-bearing sands (figure 4.10).

The effective porosity for purple part is almost zero which is an indication of shale and it can be inferred that there are only two types of lithologies in the sands of Badin reservoir. All of the cross plots confirm these results.

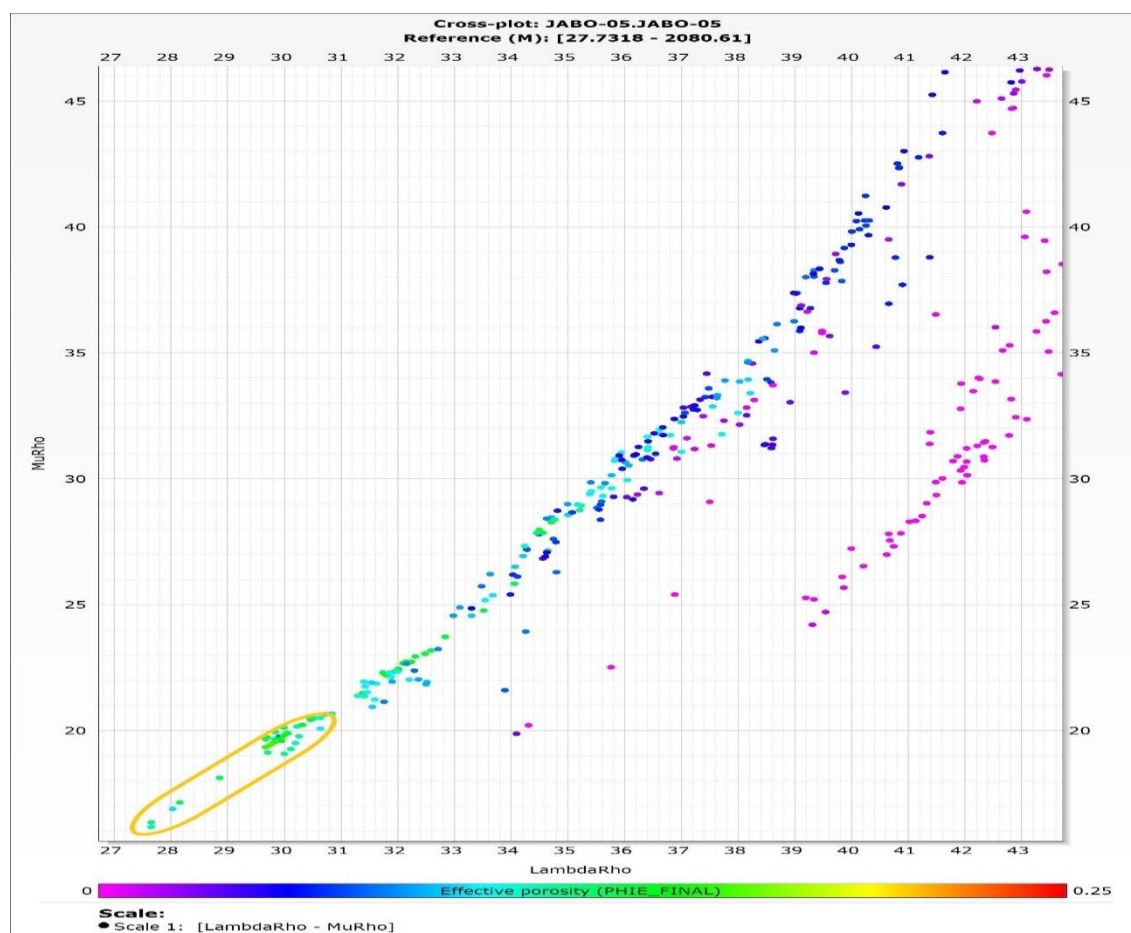


**Figure 4.10** Cross plot between MuRho and Lambda-rho for well Jabo-05. and effective porosity is shown in the color legend.

## CHAPTER 5

### SEISMIC INTERPRETATION

#### 5.1 Seismic Lines Used

On QC of data, two lines were out of the grid and were excluded for interpretation. Eight seismic lines were used for the interpretation.

**Table 5. 1** List of seismic lines.

<b>S. No</b>	<b>Lines Names</b>	<b>Lines Nature</b>
1	PK85-KH-01	Strike Line
2	PK85-KH-04	Dip Line
3	PK85-KH-06	Dip Line
4	PK85-0958	Dip Line
5	PK85-0937	Strike Line
6	PK86-1200	Dip Line
7	PK86-1202	Dip Line
8	PK92-1678	Dip Line

## **5.2 Control Line**

PK86-1200 was selected as a control line because of Jabo-01 exactly and can be easily tied to other seismic lines. At first, well data was tied to mark horizon on the control line then it was tied with other lines to mark horizons accordingly. Synthetic was also generated for this purpose.

## **5.3 Faults Interpretation**

Seismic reflections provide an indirect image and understanding of structures present in the sub-surface. Geoscientists employ their conceptual models during seismic interpretation to integrate their understandings. The marking of faults is a principle step for structural interpretation as they can act as traps for the accumulation of hydrocarbons (OXY, 1984). Faults are marked by identifying breakdown or discontinuity in strong reflectors or horizons. As stated earlier, the research area lies in an extensional regime having normal faults collectively forming horst and graben structures (Ahmed et al., 2014).

## **5.4 Horizon Interpretation**

Sub-surface events should be understood in detail so that structures favoring hydrocarbon accumulation can be identified. Traps can be structural and stratigraphic (Coffen, 1984). The stratigraphic analysis is done by marking strong and continuous reflectors across the seismic section. These reflectors are marked as formation tops aided

by well data for the well-controlled sections. Horizons can be named as respective formations from well tops.

In this research well Jabo-01 was used for the identification of formation tops on the seismic sections. A total of 5 horizons were picked in the seismic lines. Manual mode picking of horizons was used in the areas of distortion otherwise auto-tracking was used. Interpreted horizons are as following:

- 1) Lower Ranikot
- 2) Khadro Basalt
- 3) Parh Limestone
- 4) Upper Goru
- 5) Lower Goru

## **5.5 Seismic Line Interpretation**

Control line PK86-1200 (figure 5.2) was used for the stratigraphic interpretation as Jabo-01 is on the line. A synthetic seismogram was generated for this well. As the TD of both wells is in Lower Goru Formation so it is the deepest interpreted horizon.

All 5 horizons were picked on all seismic sections and there were very few regional faults associated with these horizons. All horizons can be observed straight on the seismic line GPK85-0937 (figure 5.7). As the area of research lies in the extensional regime which is confirmed by the normal faults along with horst and graben structures is the seismic lines (figure 5.4, 5.6, & 5.9).

Most of the regional faults rise from the older and deeper Lower Goru Formation to the succeeding Upper Goru Formation. Upper stratigraphic units are comparatively



much less faulted which is an indication of break or slowness of tectonic activity during their deposition.

The regional fault with a relatively higher throw on the west part of the Line PK86-1202 (figure 5.6) can be observed in other lines with progressively deepening westwards direction. Some of the faults that were correlated on the other lines are represented by different colors except black which represents non-relatable faults. Lower Goru is the reservoir in the region as the TD of the wells also lies in the Formation and Jabo-01 can be observed penetrating the horizon at about 1480 m (figure 5.2).

## **5.6 Synthetic Seismogram**

A synthetic Seismogram was developed on the well Jabo-01 for the confirmation of horizons. Gamma-ray, density, and sonic logs along with provided TD charts were used for the generation of the synthetic seismogram. It can be seen in figure (5.1) and synthetic to seismic tie is shown in figure (5.2).

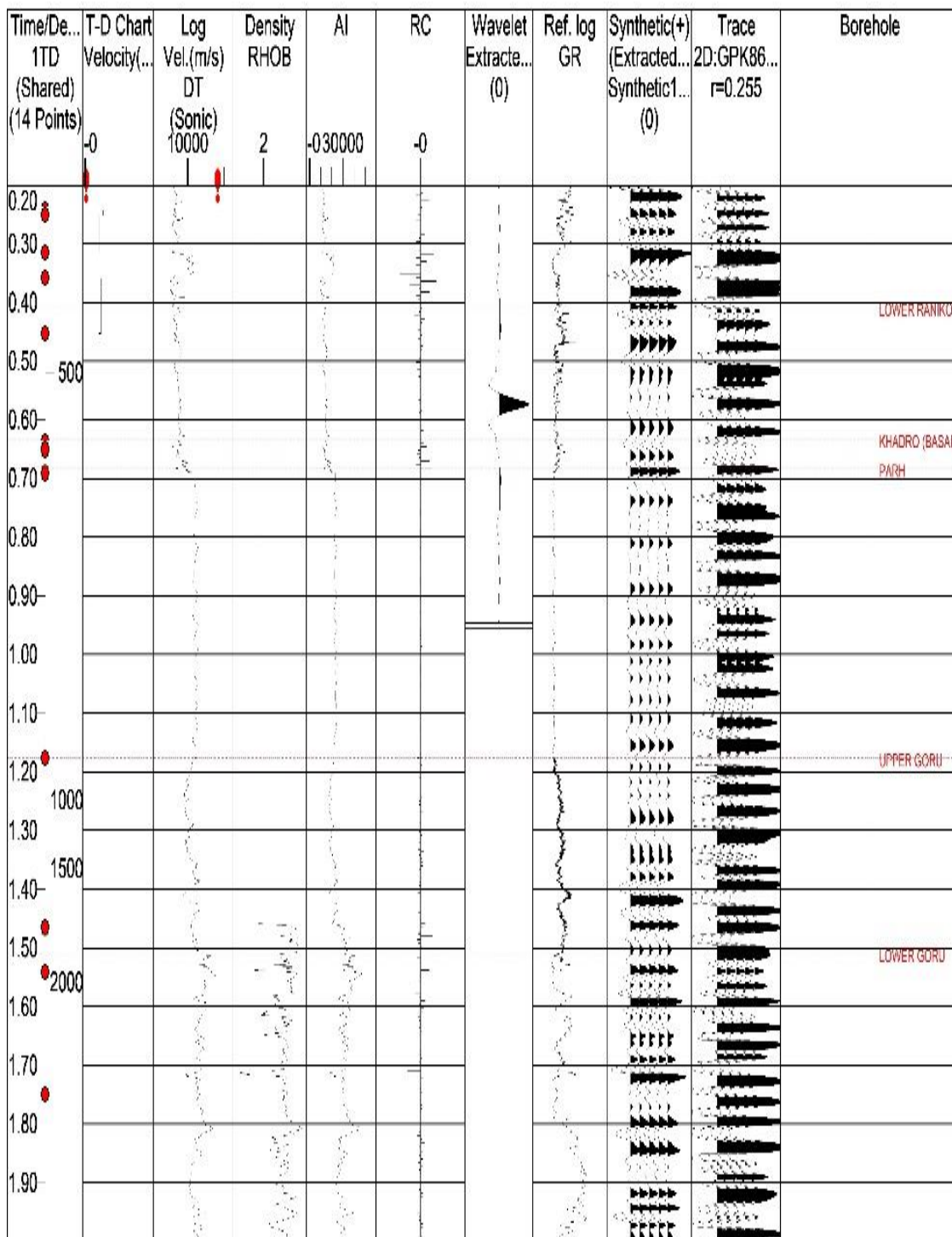
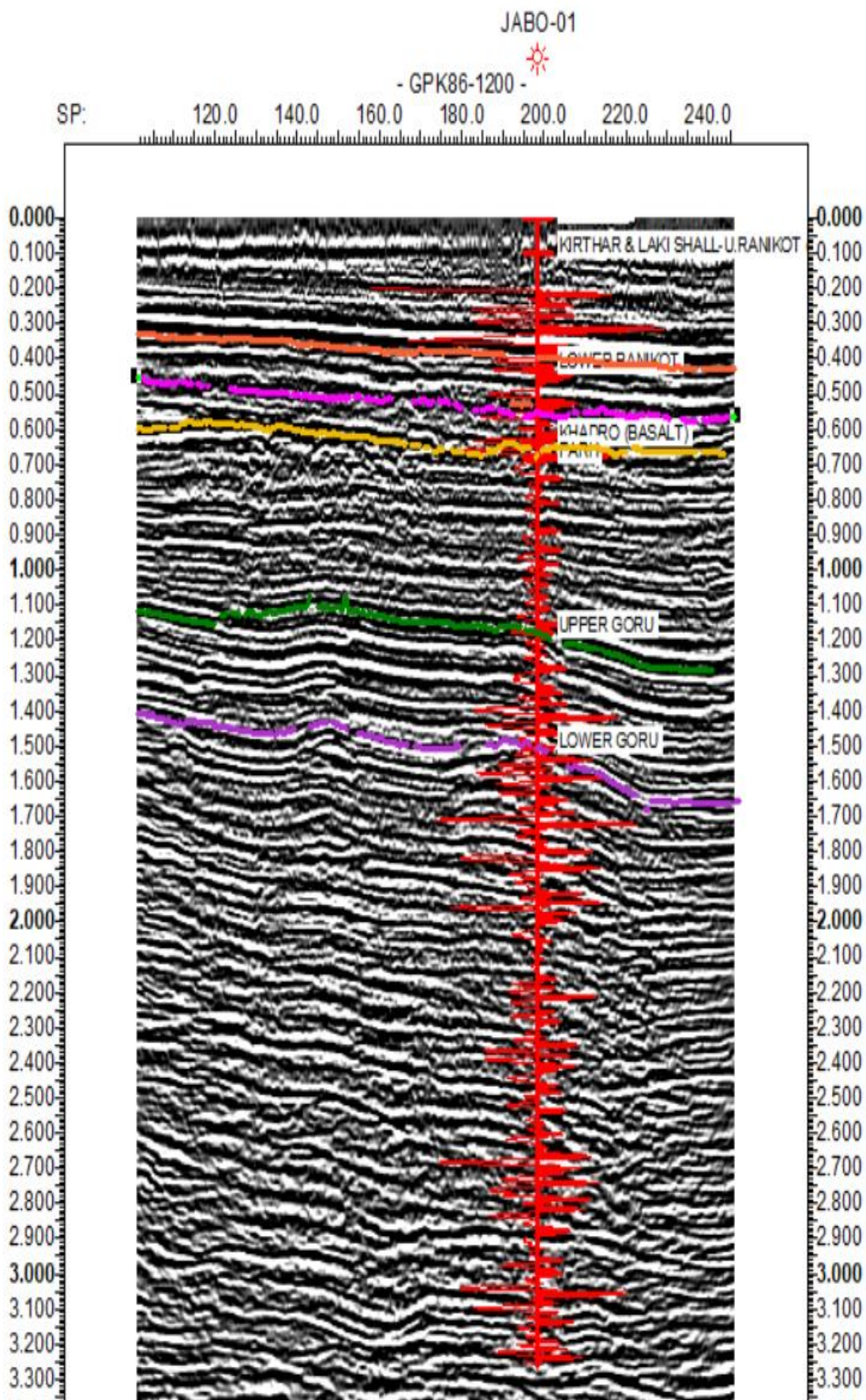


Figure 5.1 Synthetic seismogram in Jabo-01



**Figure 5.2** Synthetic to seismic tie on line GPK86-1200.

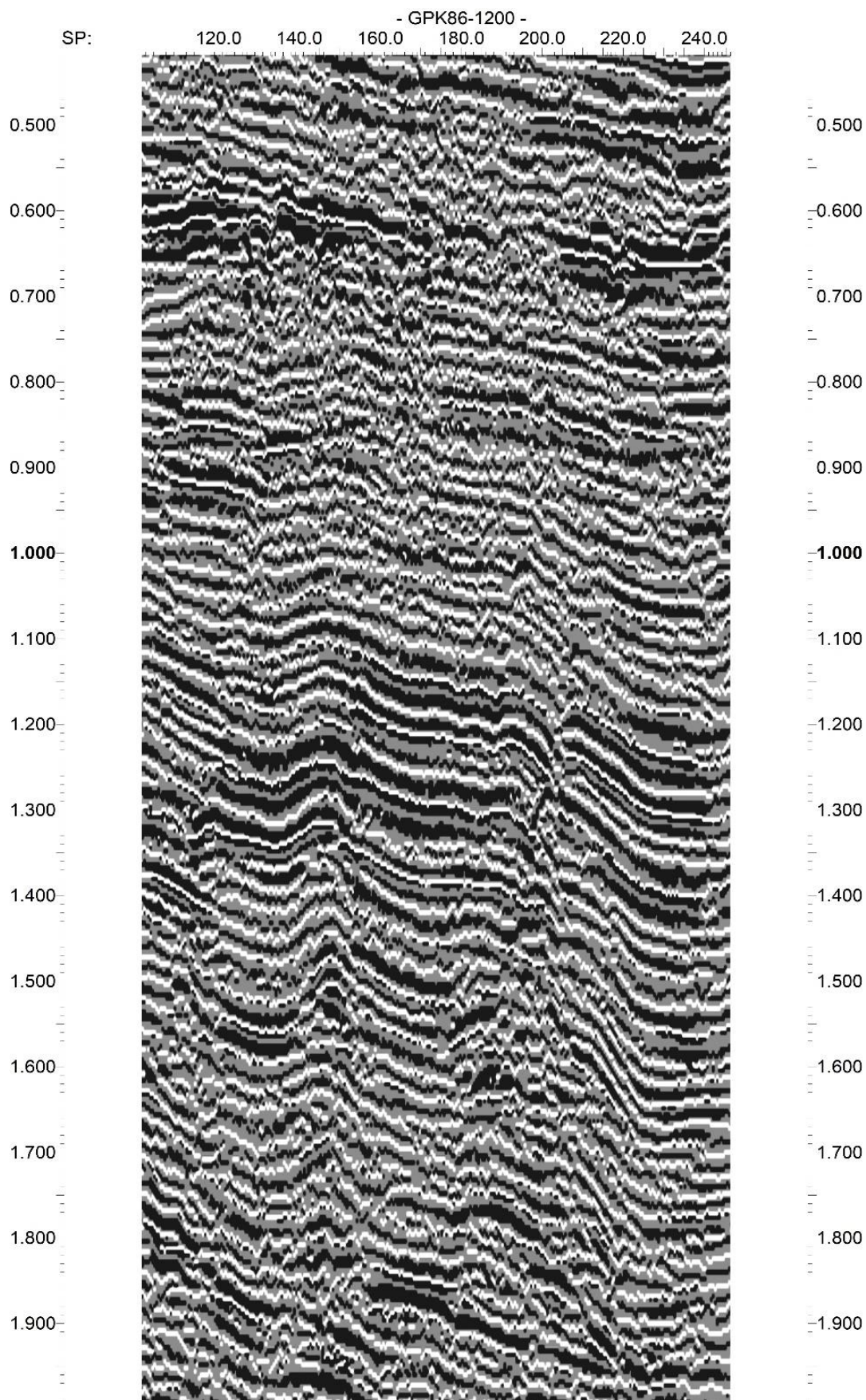
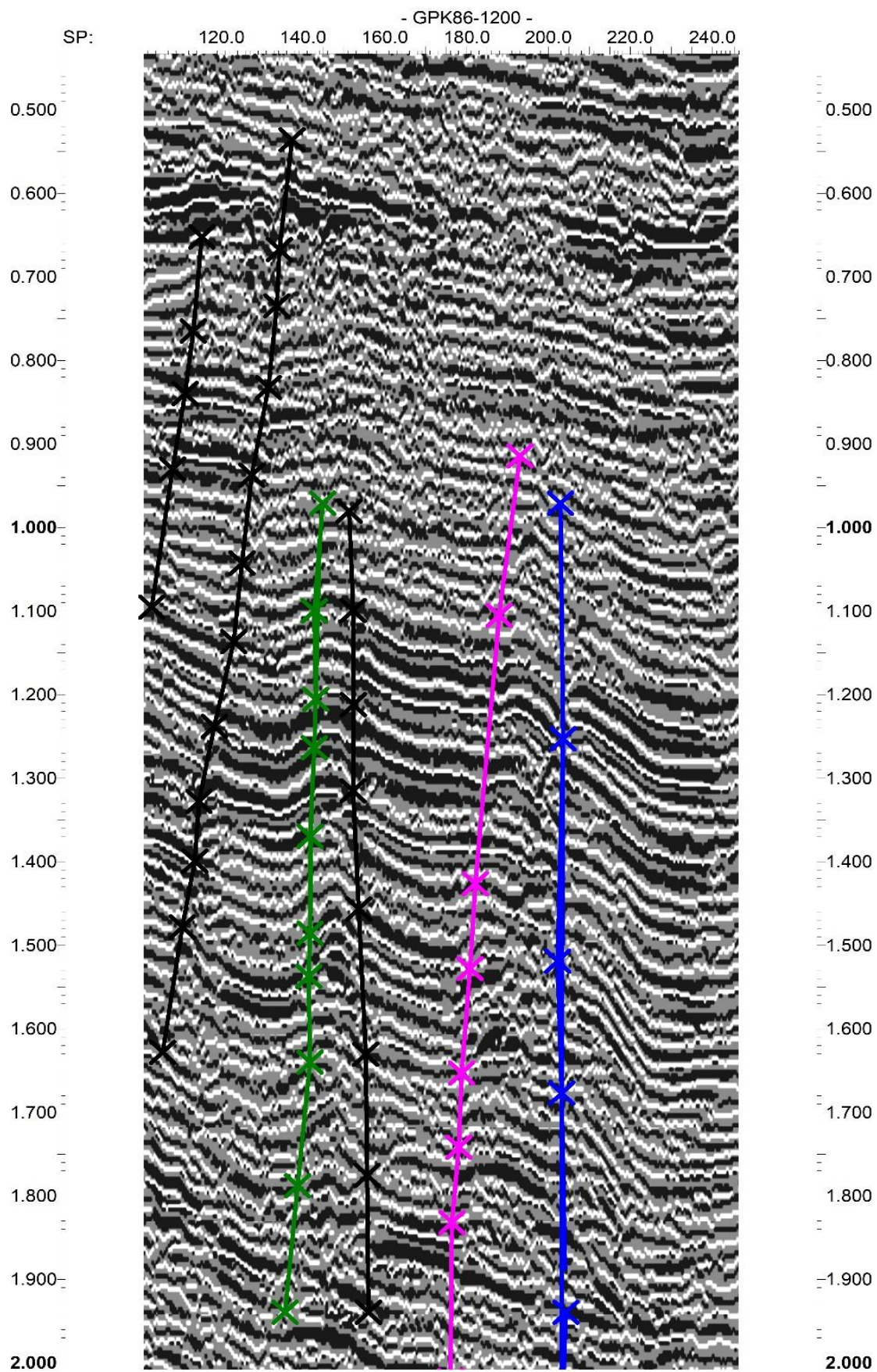
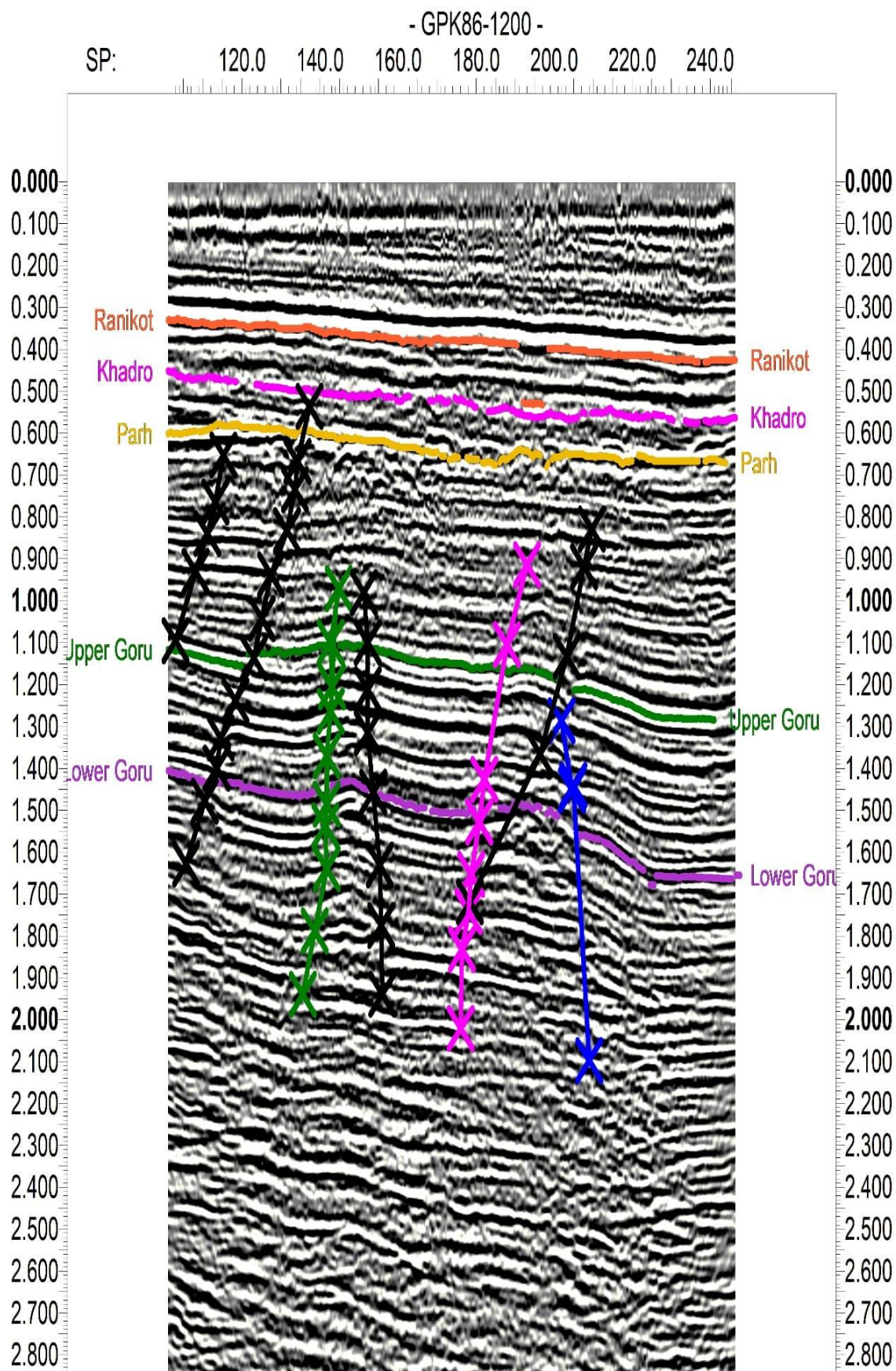


Figure 5.3 Seismic line GPK86-1200.



**Figure 5.4** Structural interpretation of seismic line GPK86-1200.



**Figure 5.5** Structural and stratigraphic interpretation of seismic section GPK86-1200.

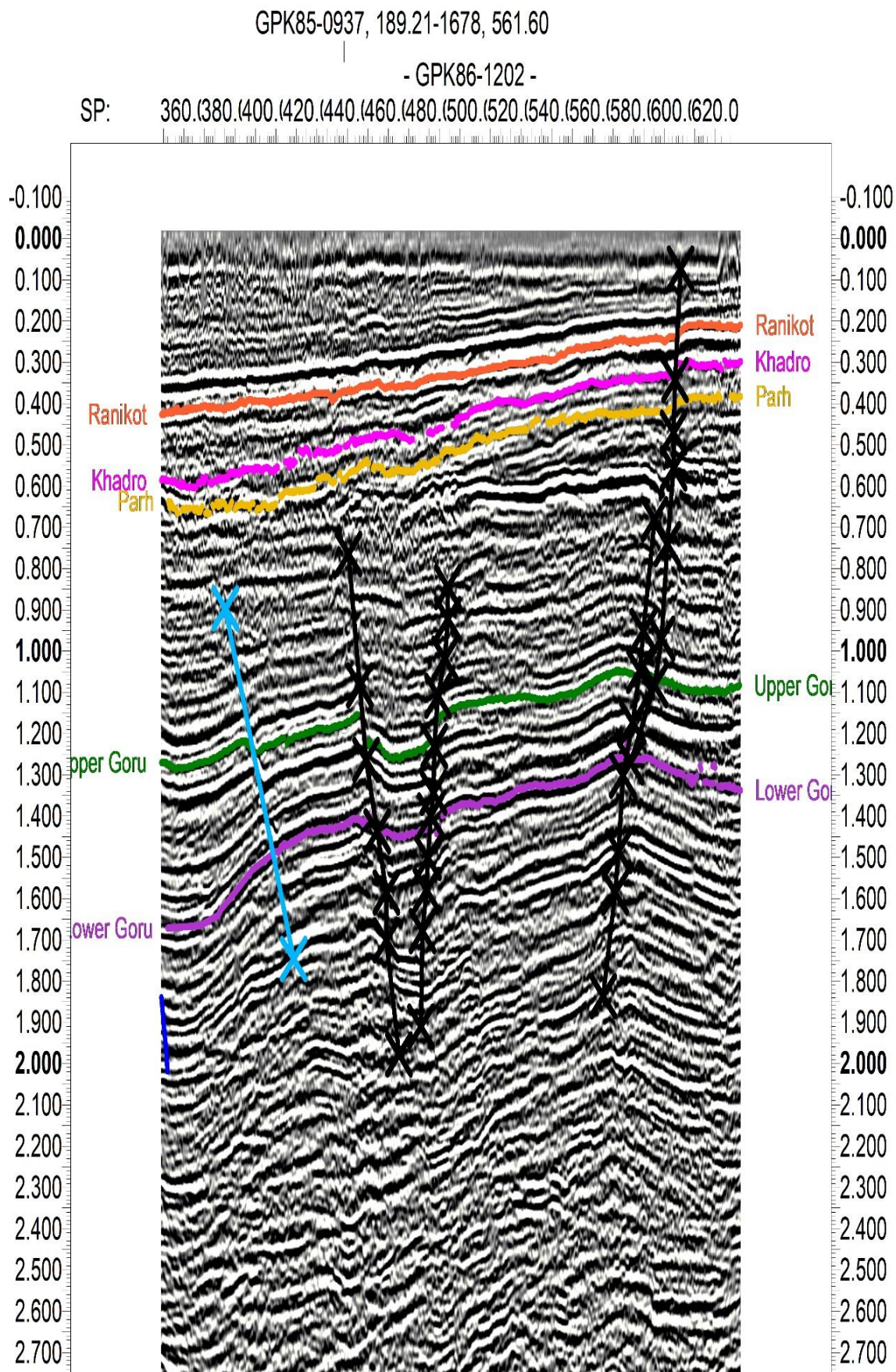


Figure 5.6 Interpreted seismic line GPK86-1202.

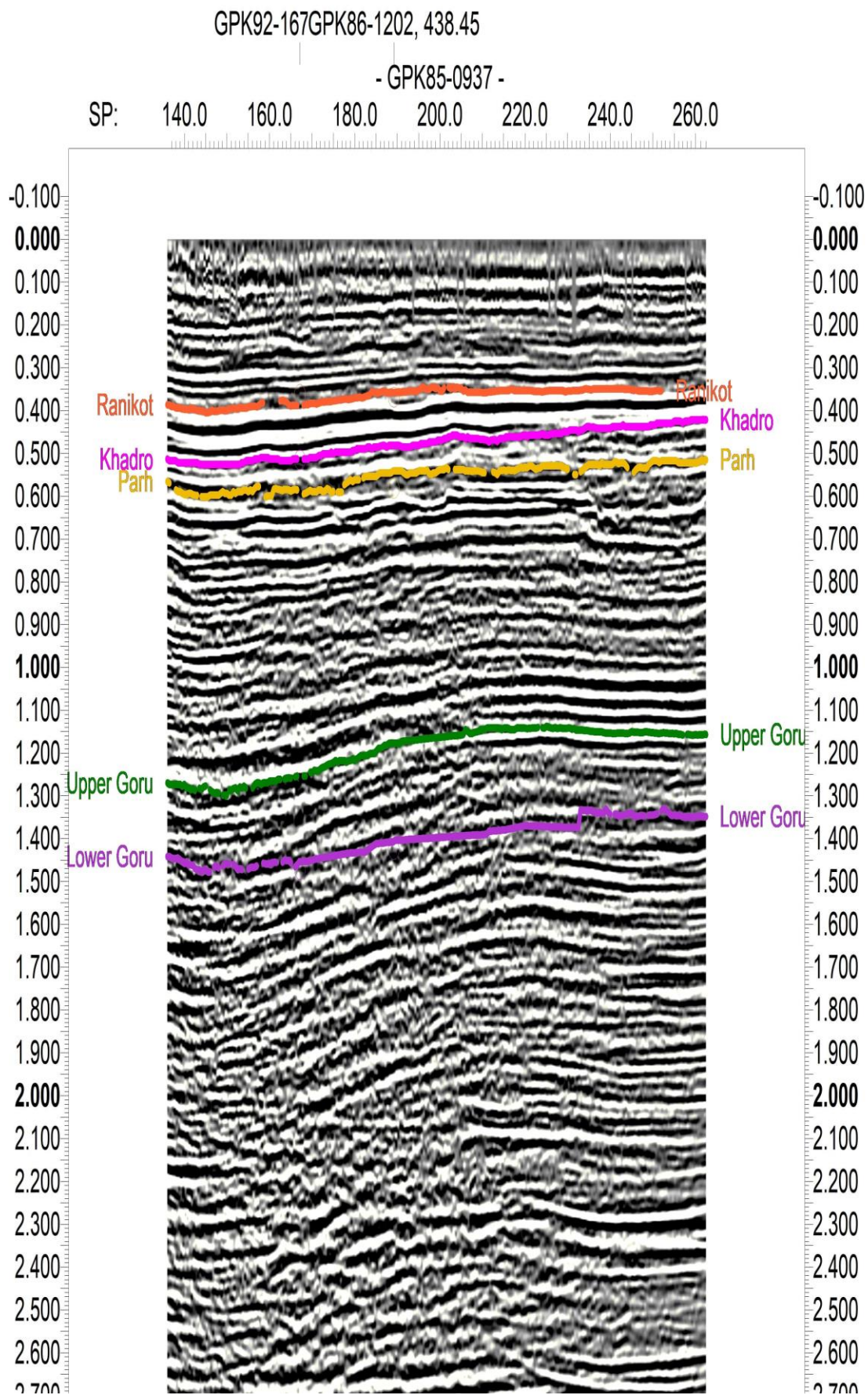


Figure 5.7 Interpreted seismic line GPK85-937.



GPK85-KH01, 107.14

- GPK85-0958 -

SP: 120.C140.C160.C180.C200.C220.C240.C260.C280.C300.C320.C340.C360.0

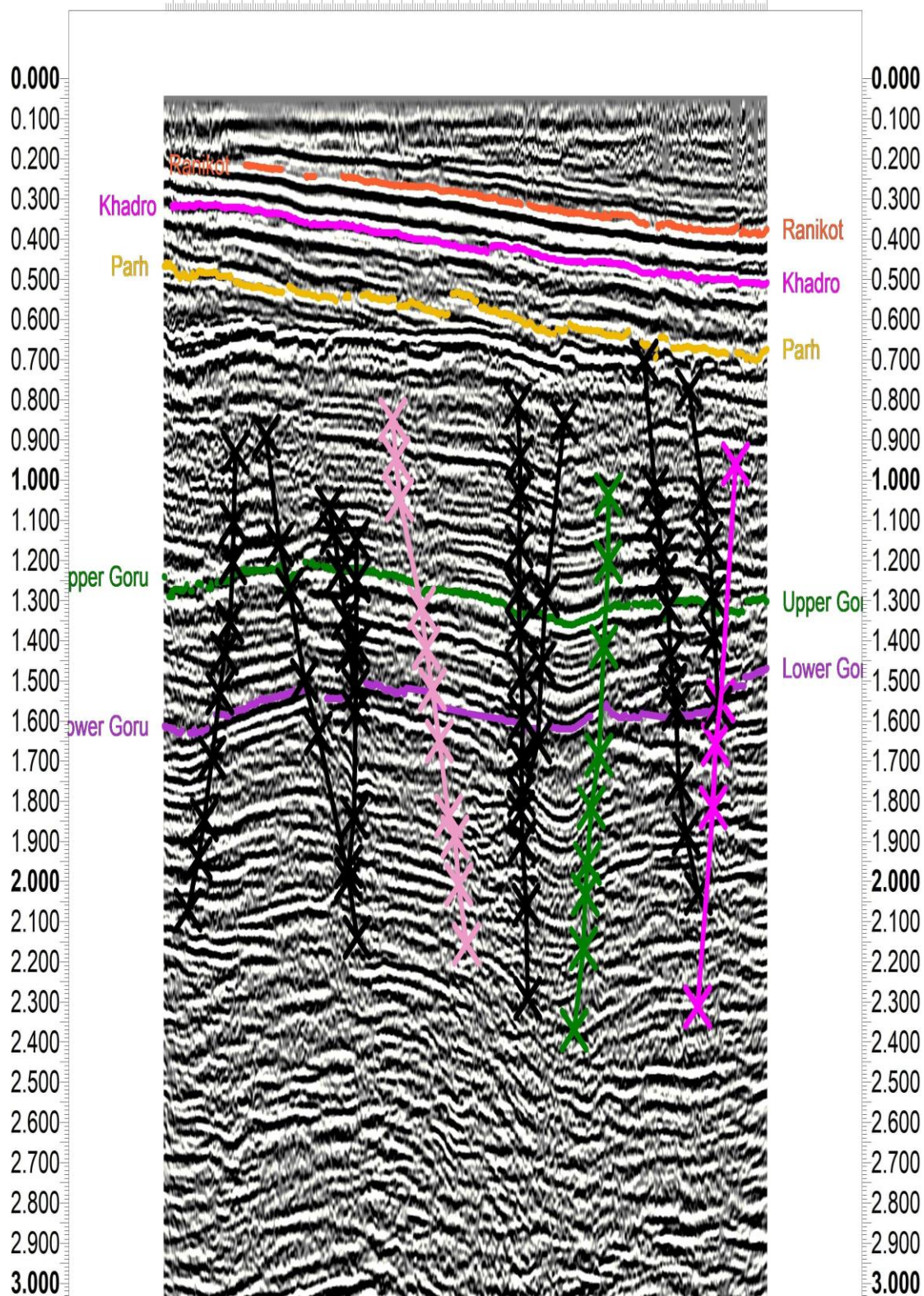


Figure 5.8 Interpreted seismic line GPK85-958.

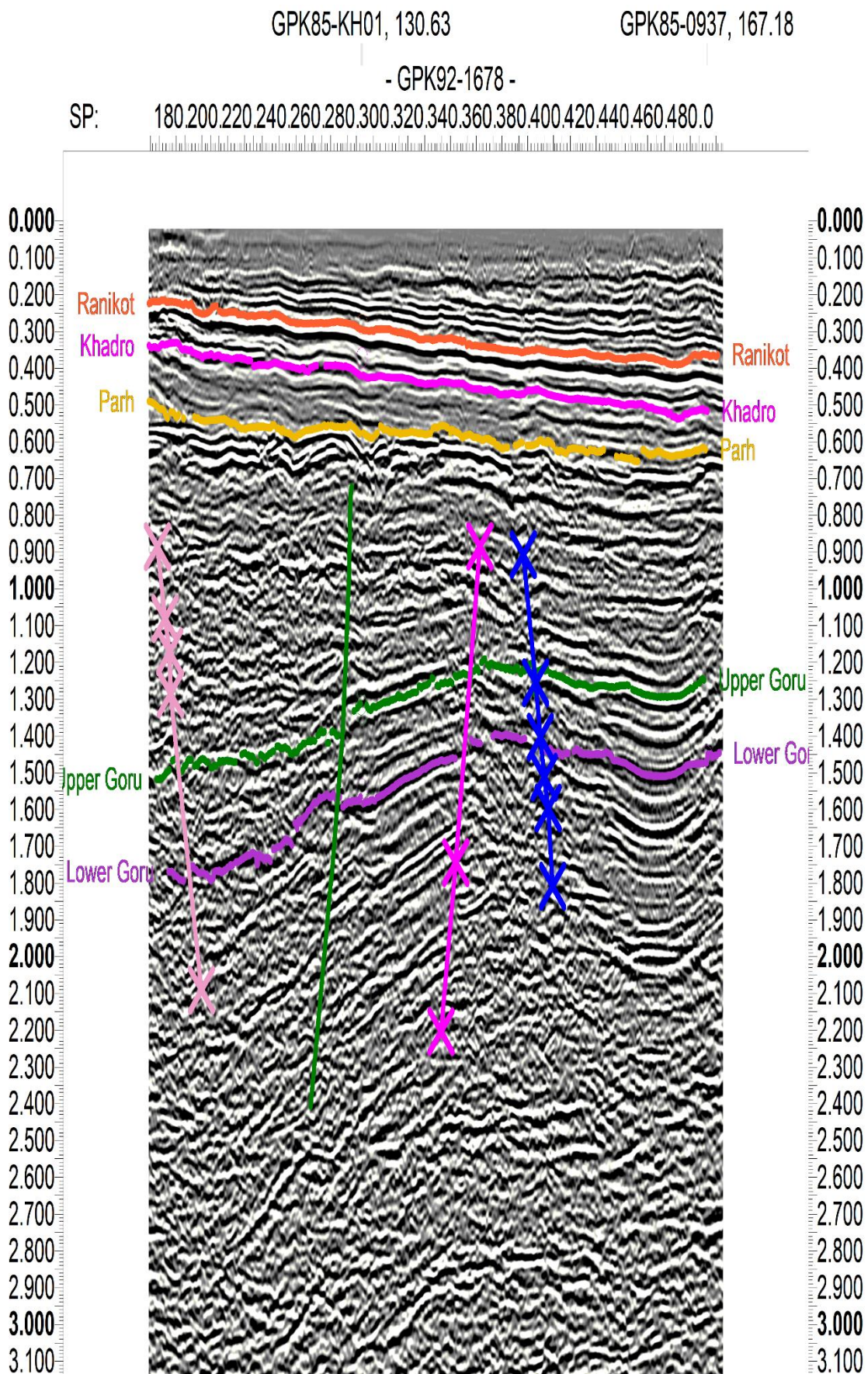
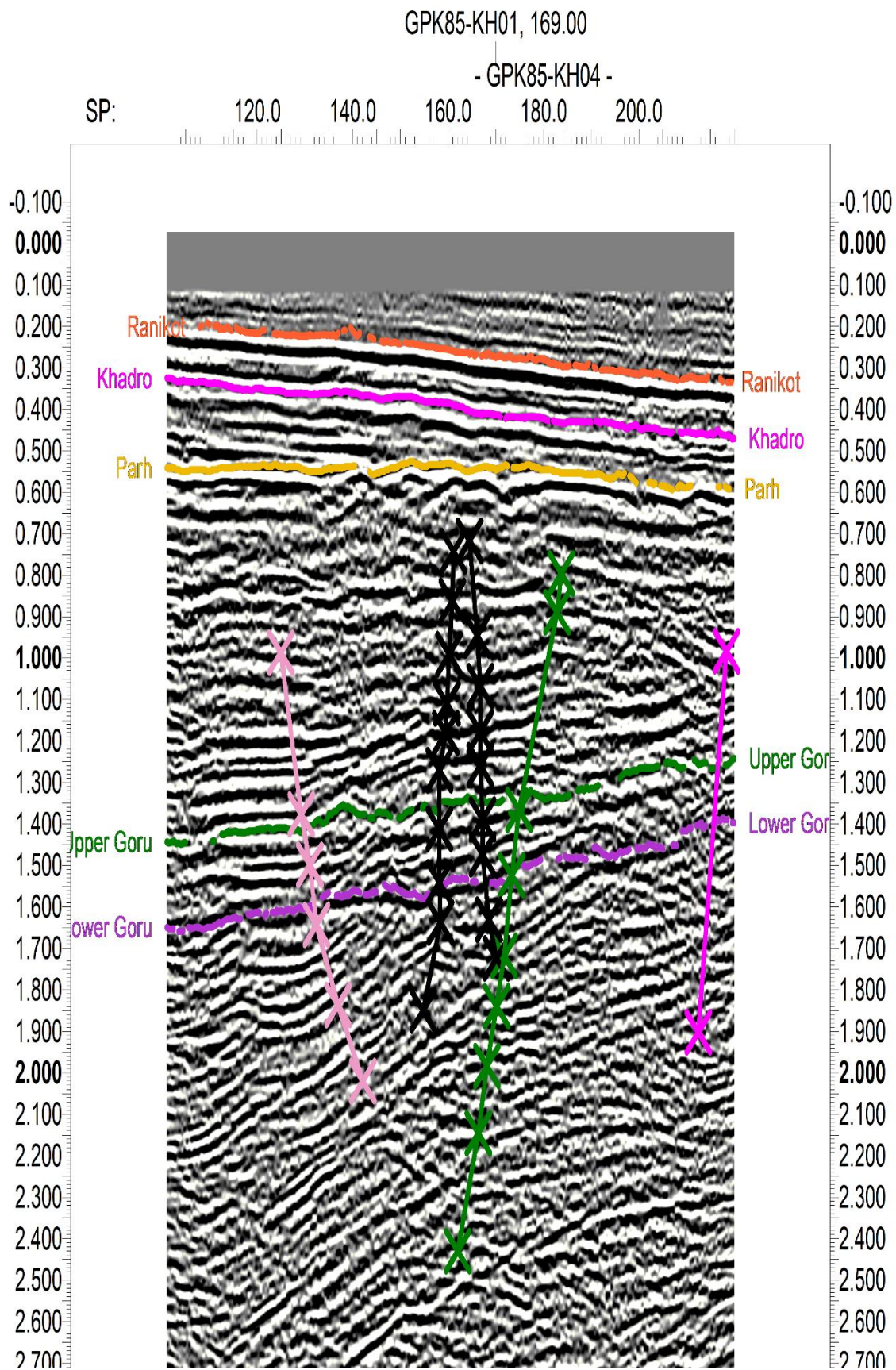


Figure 5.9 Interpreted seismic line GPK92-1678.



**Figure 5.10** Interpreted seismic line GPK85-KH04.

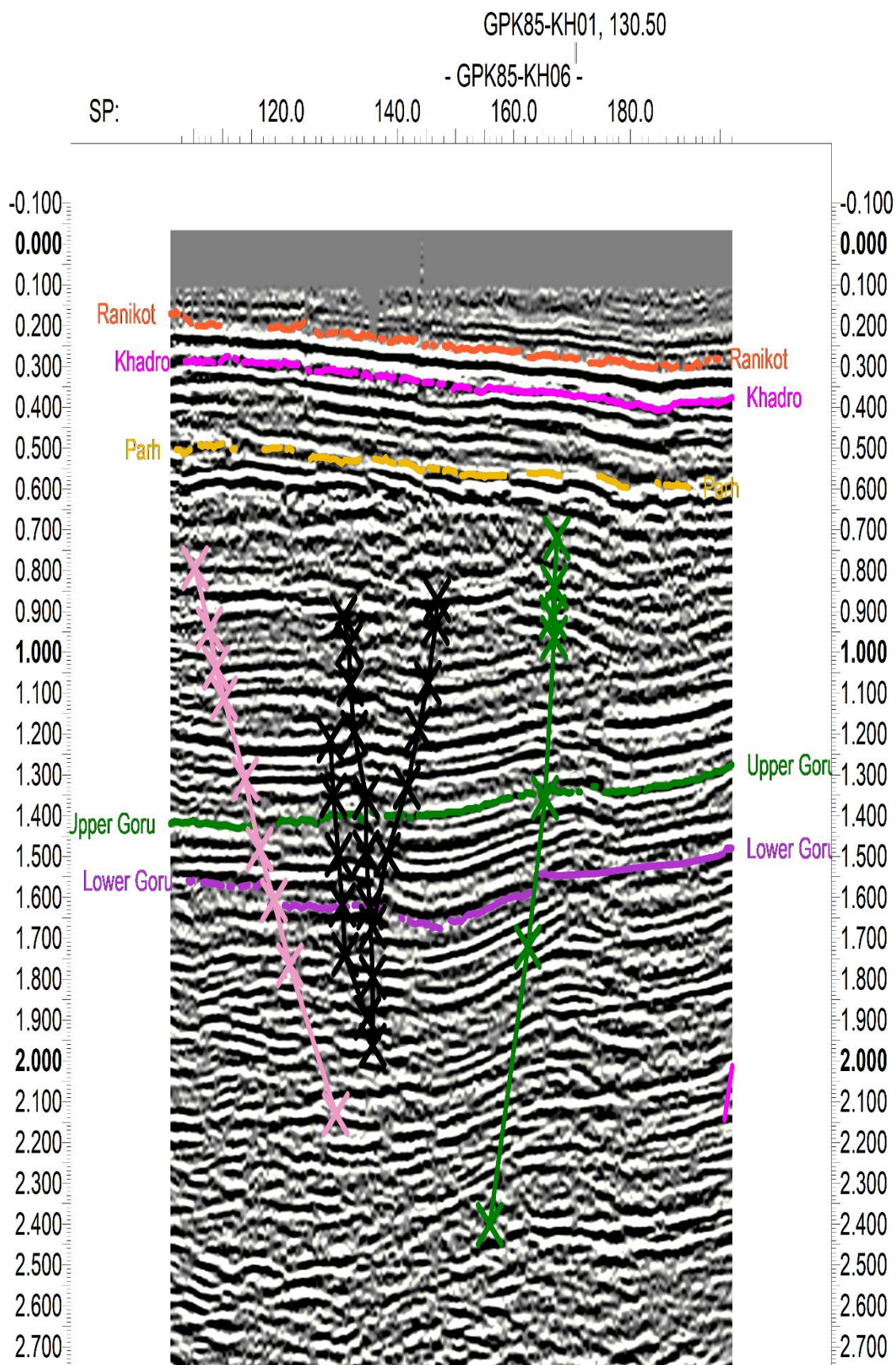


Figure 5.11 Interpreted seismic line GPK85-KH06.

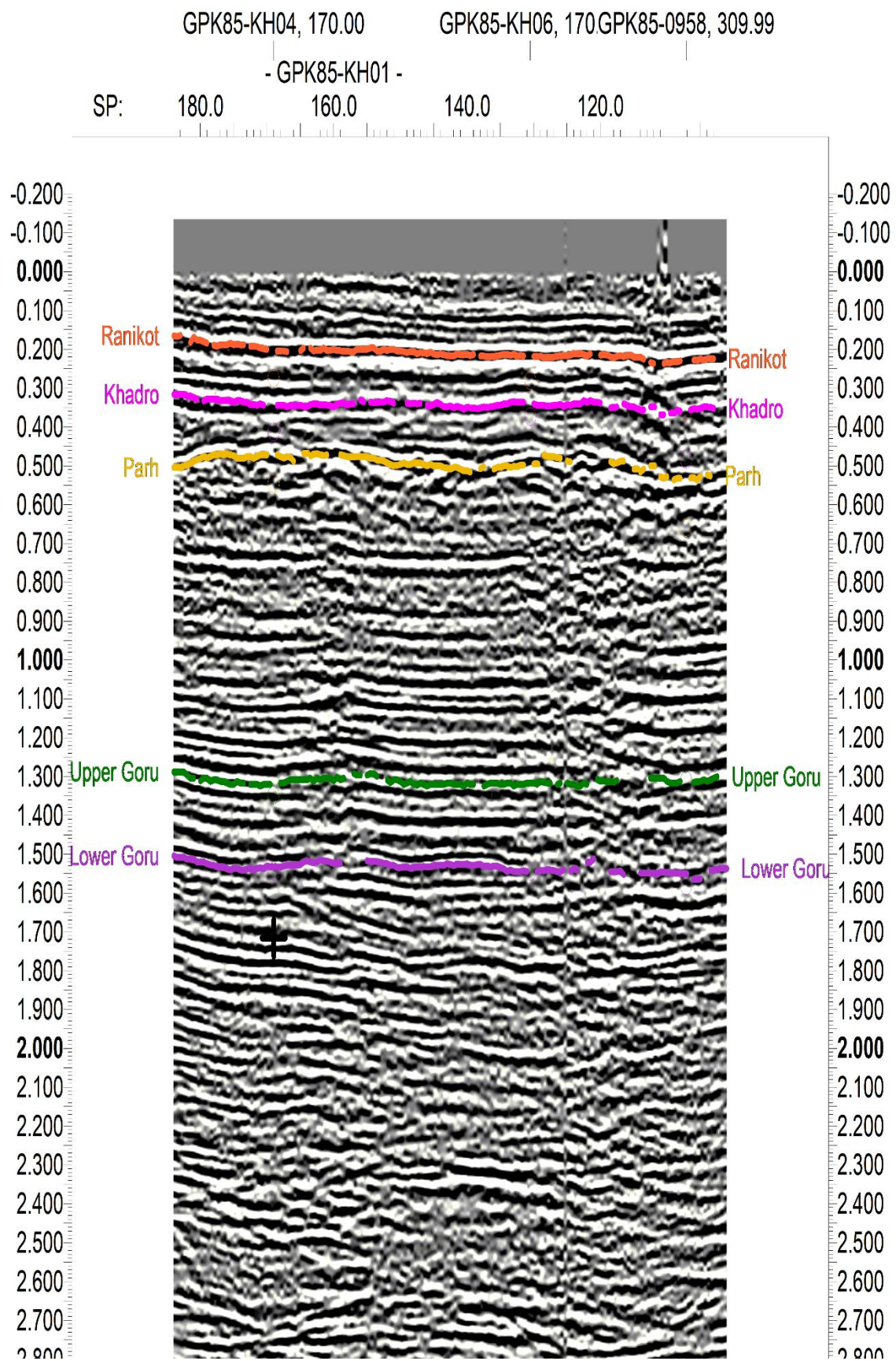


Figure 5.12 Interpreted seismic line GPK85-KH01.

## **5.7 Contour Maps**

### **5.7.1 Time Contour Maps**

Two types of maps were generated for two horizons by using the Mean Sea level as the reference datum.

### **5.7.2 Depth Contour Maps**

Depth contour maps are a visual representation of the physical existence of horizons. Check shot data from the well Jabo-01 was used for conversion of time to depth.

## **5.8 Contour Maps Interpretation**

Observations from the contour maps of horizons are as follows.

### **5.8.1 Top Upper Goru Formation**

Its reflectors were easy to pick on all of the seismic lines. Structurally this horizon is highly faulted emerging from deeper stratigraphic sections in all of the seismic sections.

Two regional faults with higher throw were observed in the middle section of maps dipping southeast (figure 5.12 & 5.13). Faults marked on the sections for Upper Goru are mostly normal faults. Localized horst and graben were also observed and can be seen in the central portion.

The stratigraphic unit is dipping in the southeast direction which can be seen in time and depth contour maps (figure 5.12 & 5.13).

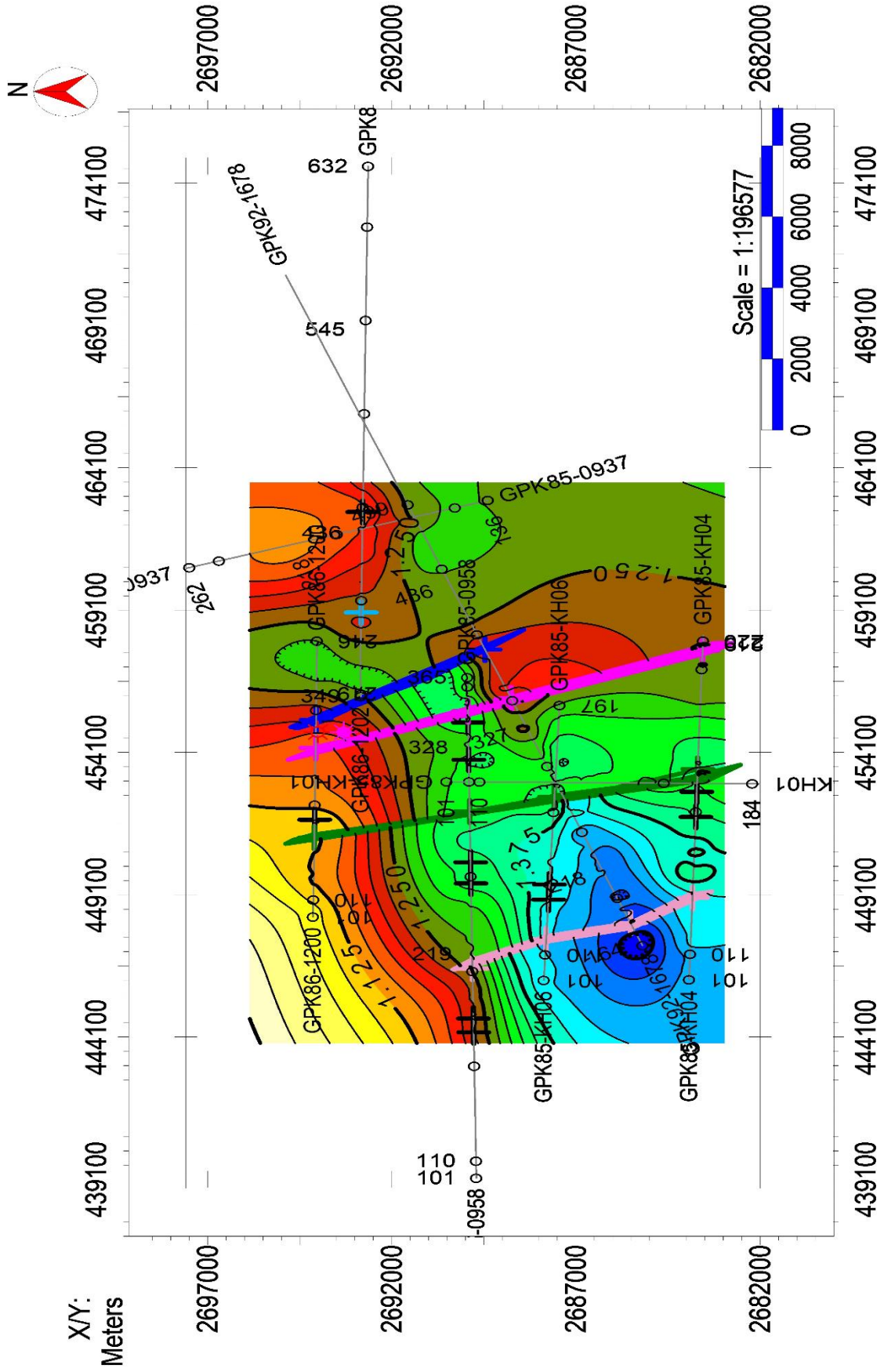


Figure 5.13 Time contour map of Upper Goru Formation.



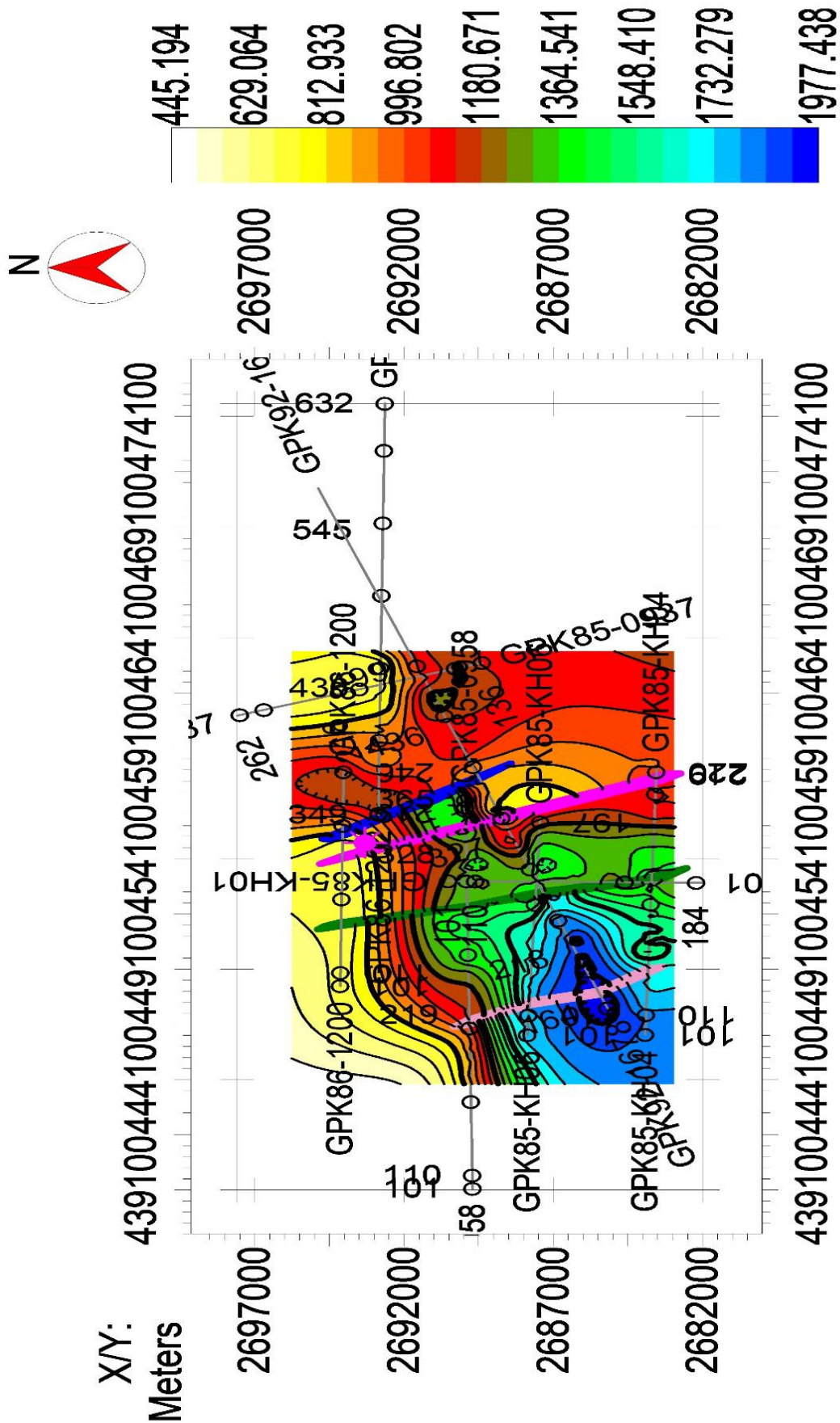


Figure 5.14 Depth contour map of Upper Goru Formation.

### 5.8.2 Top Lower Goru

This horizon was prominent on the available seismic lines and was easily marked with aid of well data. It can be observed that this lithological unit is dipping towards the southeast direction (figure 5.14).

Structural interpretation confirms that it's highly faulted in the region. Intense faulting can be seen in interpreted seismic line GPK86-1202 (figure 5.6) but its intensity is lower on the other sections. Two regional faults can be seen with dipping southeast in maps (figure 5.14).

The existing structure of this reservoir is bounded by a fault system on one side and by dips on all remaining sides. It is a structurally stable reservoir and can accumulate hydrocarbons as it is also verified by the production of oil and gas from both wells. As currently Jabo-01 is abandoned while Jabo-05 is still producing.

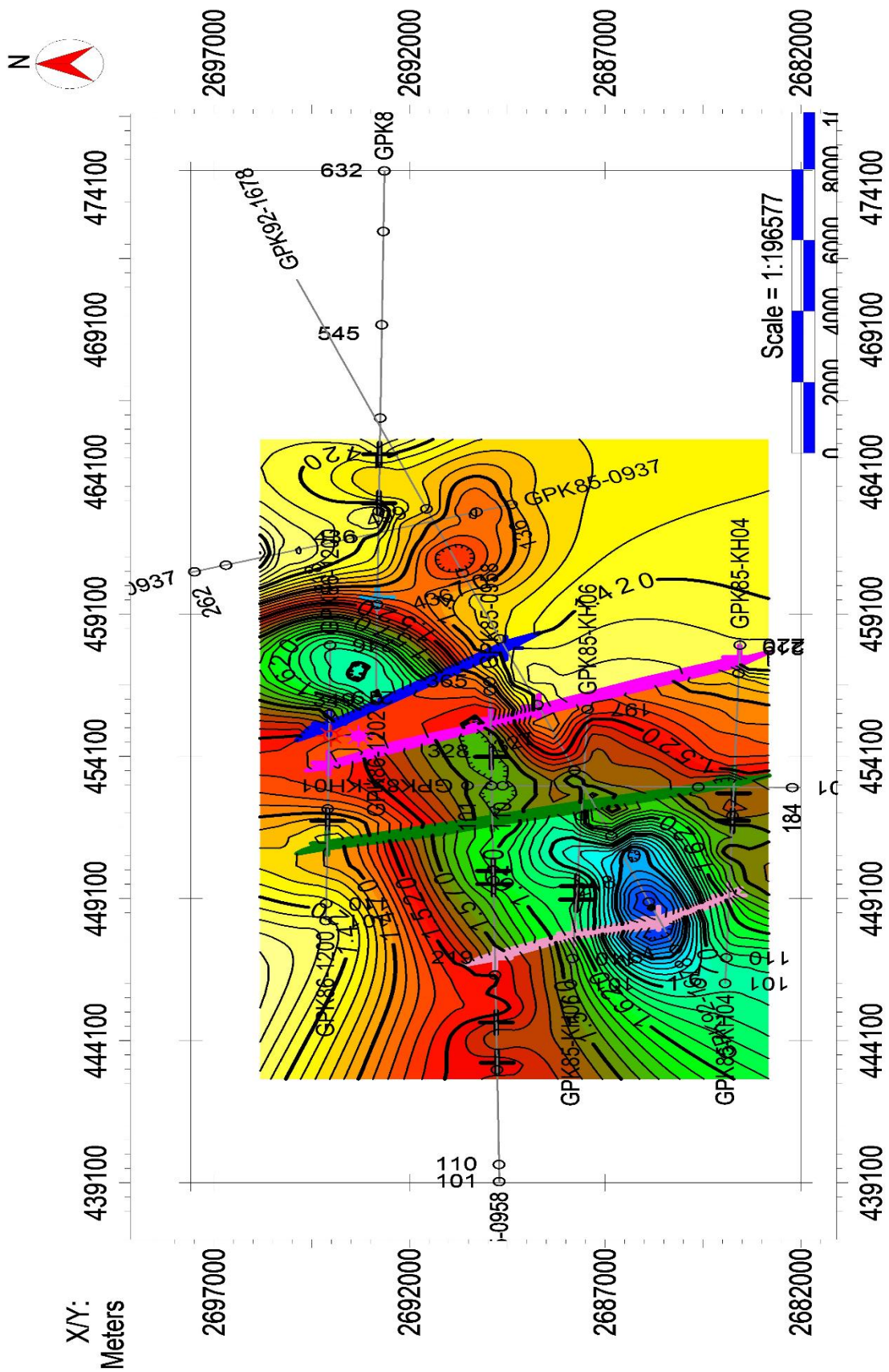


Figure 5.15 Time contour map of Lower Goru Formation.

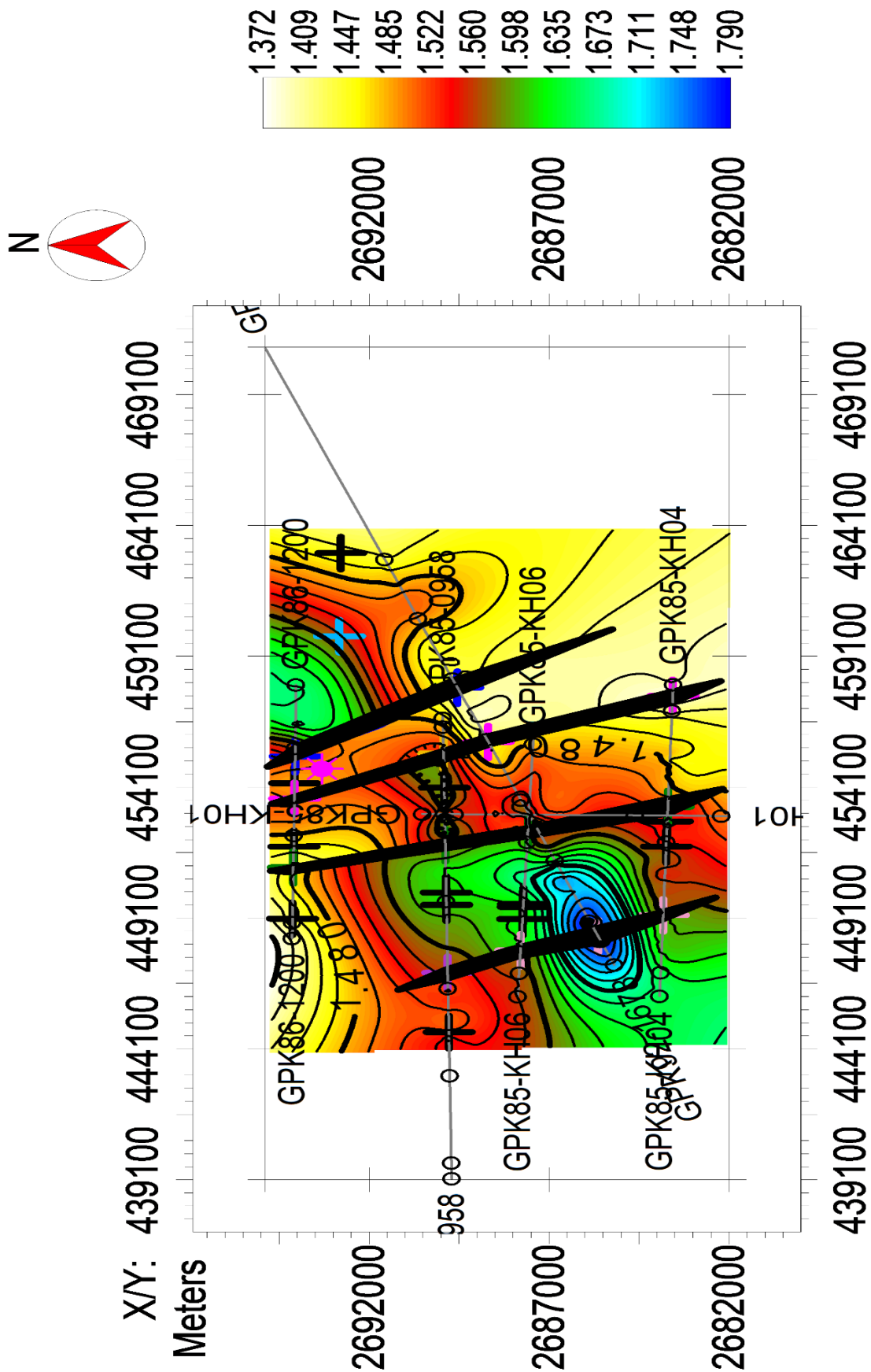


Figure 5.16 Depth contour map of Lower Goru Formation.

## CONCLUSIONS

This research leads to the following conclusions:

1. The upper sands of the Lower Goru Formation were deposited in shallow marine shelf deposition, transgressive marine, beach and barrier bar, and shore face environment of deposition.
2. The petrophysical analysis shows that Lower Goru Formation has effective porosity ranging from 5% to 8.6% with sandstone ranging from 55% to 60%. This indicates that the Jabo field has an increasing reservoir porosity trend in the southern direction.
3. Water saturation is higher on the northern side of the field while hydrocarbon saturation is higher towards the southern part of the field.
4. Structural interpretation revealed the presence of normal faults in the study area. Series of normal faults collectively led to the formation of horst and graben structures. The fault's orientation is northwest and southeast.
5. It is revealed that this region has undergone extensive deformation along with depositional changes which are confirmed by the presence of normal faults along with horst and graben structures up to the Cretaceous Upper Goru Formation while overlying units are not affected.
6. The Petroleum system of the area is aided by fault structures in the subsurface as faults are acting as traps for the accumulation.

7. Contour maps indicate that reservoir in the Badin area is dipping in the southeast direction.

## REFERENCES

- Ahmed et al., (2004). *Sequence Stratigraphy as a predictive tool in Lower Goru Fairway, Lower and Middle Indus Platform, Pakistan*, Annual Technical Conference, 85-93.
- Ahmed et al., (1999). *Study on oil and gas distribution in the Badin Block: Union Texas Pakistan, Inc.*, SPE-PAPG, Annual Technical Conference, 137-147.
- Ahmed, et al., (2014). *Study of Stratigraphy and Structural Styles in the Subsurface of Southern Sindh Monocline, Pakistan: Using Seismic and Well Data*. Sindh University Research Journal (Science Series), 46, 439-446.
- Ahmed et al., (2018). *Tectonic evolution of structures in Southern Sindh Monocline, Indus Basin, Pakistan formed in multi-extensional tectonic episodes of Indian Plate*. Geodesy and Geodynamics, 9(5), 358-366.
- Boyd, (1994). *Hydrocarbon Generation, Migration, and Expulsion within the Badin concession, Lower Indus Basin*. UTP-D-T, 2, 85-86.
- Coffen J. A. (1984). *Interpreting Seismic Data*. Penwell Publishing Company, Tulsa, Oklahoma. 39-118.
- Das, B., & Chatterjee, R. (2018). *Well log data analysis for lithology and fluid identification in Krishna-Godavari Basin, India*. Arabian Journal Of Geosciences, 11(10)

- Ebdon et al., (2012). *Sequence stratigraphy of the B Sand (Upper Sand, Lower Goru Formation) in the Badin area, Implications for development and exploitation: PAPG/SPE Annual Technical Conference*, 8-9.
- Golyan and Fardi. (2012). *Compaction, rock property evolution and rock physics diagnostics of Askeladd discovery, Norwegian Barents Sea, University of Oslo (MS)*.
- Raza et al., (1990), *Petroleum geology of Kirthar sub-basin and part of Kutch basin: Pakistan Journal of Hydrocarbon Research*, 1, 29–74.
- Hanif, et al., (2012). *Integrated stratigraphy and paleoenvironment of the P/E boundary interval, Rakhi Nala section, Indus Basin (Pakistan)*. *Arabian Journal of Geosciences*. 7(1), 323-339.
- Hargreave, (1990). *Oil and Gas Generation within the Badin Block, Volumetrics and Recommendations for future Exploration Indus Basin*. UTP-T-J, 1, 24.
- Hedley. R. et al., (2001). *Sequence Stratigraphy & Tectonics in the Kirther Foldbelt, Pakistan*. SPE Annual Technical Conference, 61-70.
- HDIP. (2019). *Pakistan energy yearbook 2016*, Islamabad, 1-145.
- Kadri, I. B. (1995), *Petroleum geology of Pakistan, Pakistan Petroleum Limited*, 274-275.
- Kazmi, A.H, and Jan, M.Q. (1997). *Geology and Tectonics of Pakistan*. Graphic publishers Karachi, Pakistan.
- Kemal, A., (1992). *Geology and new trends for petroleum exploration in Pakistan*. International petroleum seminar, Ministry of Petroleum and Natural Resources, Islamabad, Pakistan, November, 16-57.
- Kennedy, M. (2015). *Developments in petroleum science, Practical Petrophysics*. Elsevier, 62.



- Kumar, et al., (2017). *Petrophysical evaluation of well log data and rock physics modeling for characterization of Eocene reservoir in Chandmari oil field of Assam-Arakan basin, India*. Journal of Petroleum Exploration and Production Technology, 8(2), 323-340.
- Memon, et al., (1988). *Tectonic of Sindh Monocline, Pakistan and their effects on hydrocarbons*, Mehran University Research Journal of Engineering and Technology, 18(10), 87-94.
- Omudu, et al., (2007). *Optimizing quantitative interpretation for reservoir characterization: Case study onshore Niger Delta*. Annual SPE International Technical Conference and Exhibition In Abuja, Nigeria, 31.
- OXY, (1984). *Pakistan Basin Task Force Report*, 4, 22-24.
- Petzet, G.A. (1997). *Union Texas hopes to reproduce its Pakistan Basin experience*. Oil and Gas Journal, November. Penwell, Tulsa, OK, United States.
- Serra, O. (1984). *Fundamentals of well-log interpretation*, 21-22.
- Shah, S. H. A. (1977). *Stratigraphy of Pakistan*, Geological Survey of Pakistan Memoir, 12, 37–150, 130-150.
- Zaigham and Mallick, (2000), *Prospect of hydrocarbon associated with fossil rift structures of the Southern Indus Basin, Pakistan*. AAPG Bulletin, 84, 11, 1833-1848.